Investigation into design and optimisation of solar adsorption cooling/air conditioning under the Iraq climate

By

Zaynab Ismail Abdullah

NO. 10514033

A thesis submitted to the Plymouth University in partial fulfilment for the degree of

Master of Philosophy

in

Mechanical Engineering

Faculty of Science and Engineering

School of Marine Science and Engineering

Plymouth University

December 2015

Investigation into design and optimisation of solar adsorption cooling/air conditioning under the Iraq climate

Abstract

Solar adsorption cooling system can be defined as a system produces a cooling effect by using Sun's thermal energy. In present study, a solar adsorption cooling system was modelled and simulated using TRNSYS and MATLAB programmes. Parametric investigations have been done on the system by varying several of the crucial design parameters, and their effects on the performance of the system were introduced. The system was analysed on the energy, exergy and economy basis, and it was further optimised by employing a multi-objective genetic algorithm technique with two objective functions. The first objective was maximising the exergy efficiency, and the second objective was minimising the total cost rate over life. The Pareto front optimal solutions that achieved from the multi-objective optimisation were presented. Moreover, Technique for Order Performance by Similarity to Ideal Solution (TOPSIS) method was applied to find the final optimal solution. The optimal design was simulated and analysed for individual components of the system. Finally, a comparison has been made with an existing solar cooling system; the comparison showed that the proposed solar adsorption system driven by evacuated tube collector, integrated with hot and cold storage tanks, has a smaller size and better performance, which in turn means less costs. The payback period method is also used in the present study. The techno-economical results showed that due to the high cost of the system and the low cost of electricity in Iraq, financial payback is not feasible, and thus would require further efforts in driving down the costs and government incentives.

List of Contents

List of Figures

List of Tables

List of symbols

A	area of the collector	m^2
C	capital cost	US$
$\dot{C}$	cost rate	US$/hr
Cp	specific heat capacity	kJ/kg .k
crf	capital recovery factor	-
Ex	exergy	kJ/hr
if	the inflation rate	-
I_T	global solar radiation	$kJ/hr.m^2$
m	mass flow rate	kg/hr
N	operation hours	hr
N_P	payback period	year
n	life span	year
PW	amortization cost	US$
Q	rate of heat transfer	kJ/hr
SF	solar fraction	-
T	temperature	K
T_o	ambient temperature	K
W	power consumption	kJ/hr
$\dot{Z}_k$	capital cost rate	US$/hr
Z_k	capital cost	US$

Subscripts

am	ambient
aux	auxiliary heater
avg	average
chill	chiller
cold_tank	cold storage tank
Ct	cooling tower
des	destruction
elec	electrical
f,ct	fan of cooling tower
hot_tank	hot storage tank
in	inlet condition
ir	interest rate
loss	losses
max	maximum
min	minimum
op	operation
out	output condition
set	set point
sol	solar
sra	solar radiation
w	water

Greek symbols

φ	specific unit exergy	kJ/kg
$\emptyset$	maintenance factor	-

μ	salvage value percentage	%
η	efficiency	%

Acknowledgement

Firstly, I would like to express my sincere gratitude to my supervisor Dr. Yong Ming Dai, for the continuous support of my MPhil study, for his patience, motivation, and immense knowledge. His guidance helped me in all the time of research and writing of this thesis. I could not have imagined having a better advisor and mentor for my MPhil study.

Besides my advisor, I owe many thanks to my lovely husband, Shahen, who gave me continuous support, and encouraging me during my study. Finally, thanks to my cute son, Adam for his patience.

Author's Declaration

At no time during the registration for the degree of Master of Philosophy has the author been registered for any other University award without prior agreement of the Graduate Sub-Committee. Work submitted for this research degree at the Plymouth University has not formed part of any other degree either at Plymouth University or at another establishment.

Word count of the thesis: 19544

Signed ……..…...

Date …18/12/2015…….

Chapter One

Introduction

1.1 Introduction

All forms of energy in the world, broadly speaking, are from the Sun in origin. Oil, natural gas, and coal were originally produced by photosynthetic processes under chemical reactions in which decaying vegetation was subjected to very high temperatures and pressures over a long period of time. This kind of energy is called fossil fuel, and since the last century fossil energy has been consumed lavishly. In the early 70s, after the oil crisis when the Arab countries stopped exporting oil to the Western countries, this led to a search for alternative energy sources (this trend retreated somewhat due to lower crude oil prices in the last two decades of the last century). The efforts of countries to promote the use of alternative energy (such as solar, wind and ocean energies) have increased due to the significant rise in the prices of crude oil after the Gulf War II, and the increasing awareness of negative effects of the emissions of greenhouse gases resulting from fossil fuel combustion, which in turn lead to environmental problems such as pollution and global warming. Because of its abundance and presence in all parts of the Earth, and its ease of harvesting and no need for transportation, solar energy can be considered as a primary source of renewables.

The amount of solar radiation that reaches the Earth's surface is high. The total solar radiation is approximately 1.74×10^{17} W (Hassan & Mohamad, 2012) and Figure 1-1 gives the annual availability of global solar radiation on the Earth.

Air conditioning and refrigeration systems play an important role in providing a comfortable environment for humans. The demand for air conditioning systems has increased significantly and continuously (Desideri, Proietti & Sdringola, 2009); for example, within the past five years the sales of air conditioning systems have doubled in China alone, and 90% of the houses in USA already have air conditioning systems (Davis & Gertler, 2015). This leads to a significant increase in energy consumption, and consequently a substantial increase in greenhouse gas emissions.

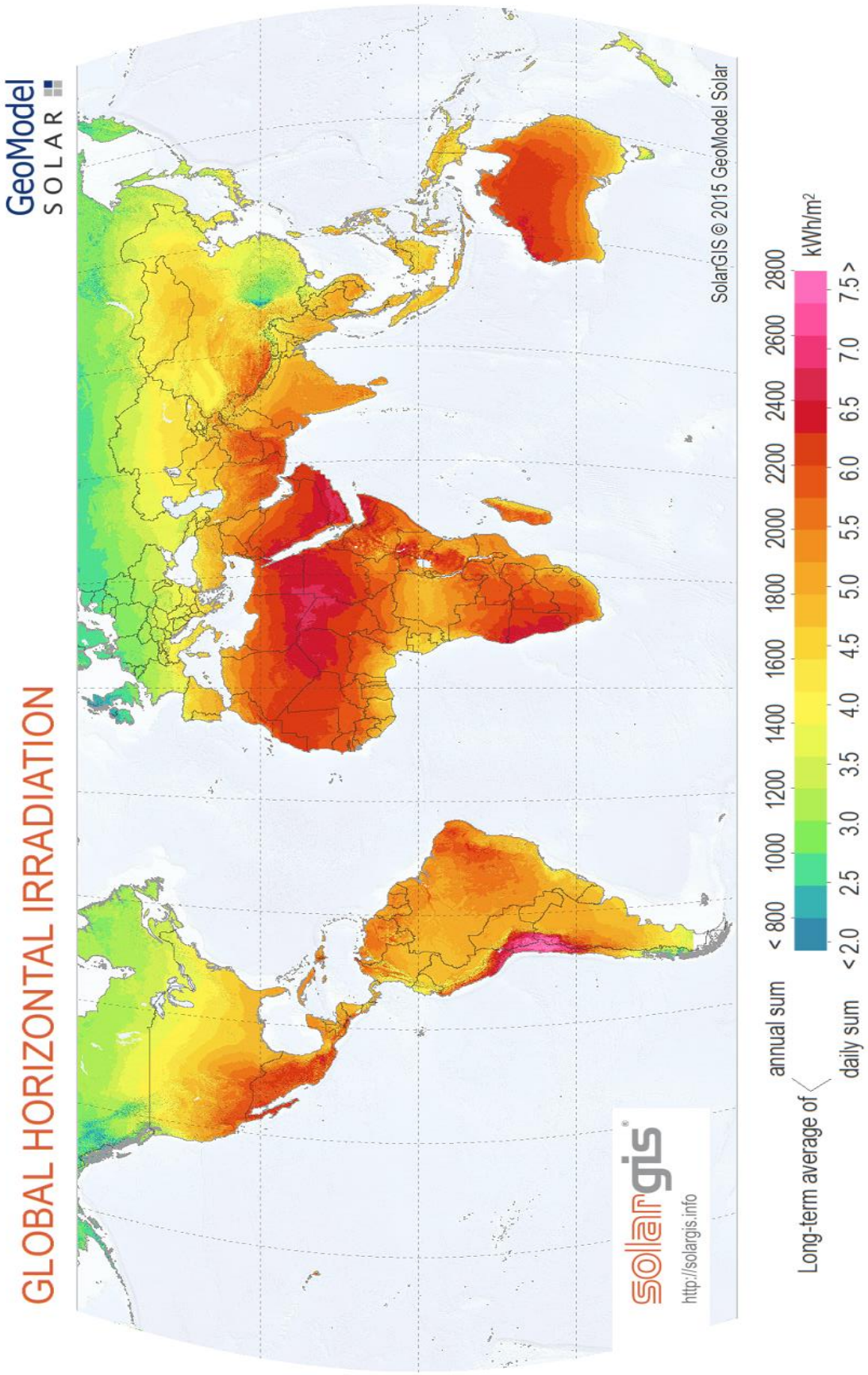

Figure 1-1 Annual average global solar radiation on a horizontal surface (kWh/m^2) ('GoModel Solar,').

In addition, the emissions of some refrigerant fluids that are used in air-conditioning systems, i.e. Chlorofluorocarbons (CFC), Hydrochlorofluorocarbons (HCFC) and Hydrofluorocarbons (HFC) have led to the depletion of the stratospheric ozone layer. Therefore, it is important to develop alternative and renewable technologies in order to provide a comfortable life for humans without harming the environment (Fong et al., 2010).

1.2 Background

Solar cooling can be defined as harvesting solar energy to produce a cooling effect by using the Sun's thermal and/or photonic energy. Solar assisted air conditioning systems are divided in to solar thermal cooling systems and solar electric cooling systems. In solar thermal cooling systems, the cooling process is driven by solar collectors collecting solar energy and converting it into thermal energy, and uses this energy to drive thermal cooling systems such as, absorption, adsorption and desiccant cycles; whereas in solar electric cooling systems, electrical energy that is provided by solar photovoltaic (PV) panels is used to drive a conventional electric vapour compressor air conditioning system (conventional mechanical system) (Baniyounes et al., 2013). Both types of solar cooling can be used in industrial and domestic refrigeration and air conditioning processes, with up to 95% saving in electricity (Desideri, Proietti & Sdringola, 2009). Solar cooling systems that utilise PV panels have low efficiencies which decrease further at high temperatures (Tyagi et al., 2013). Zhai & Wang (2009) stated that the majority of existing solar cooling systems are based on solar thermal energy because solar mechanical systems are highly expensive compared to solar cooling systems which are activated thermally. Figure 1-2 shows a simplified diagram of a thermally driven cooling chiller system using a solar thermal collector.

There are five types of solar thermal cooling (and heating) systems:- Absorption, Adsorption, Desiccant cooling, Ejector and Rankine systems (Clausse, Alam & Meunier, 2008; Ozgen, 2008). During the last three decades, there have been great efforts to use solar adsorption cooling technology since the system operates with environmentally friendly refrigerants, and thus is free from Chlorofluorocarbons (CFCs), having no ozone depletion potential (ODP) (Hassan, Mohamad & Bennacer, 2011). In addition, it can be run at a wide range of temperatures, starting from 65 °C to 500 °C, there are no moving parts in the system and no corrosion problems (Hassan & Mohamad, 2012; Wang, Wang & Oliveira, 2009).

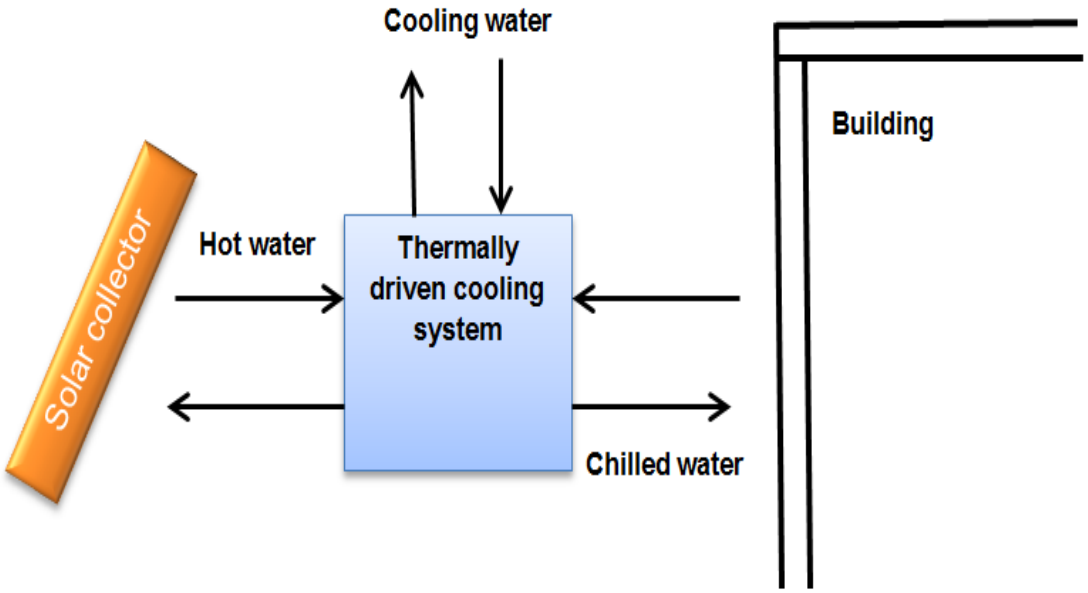

Figure 1-2 Simplified schematic of thermally driven cooling system.

Iraq is one of the Middle East countries that have a high amount of solar radiation 6.5-7 kWh/m², and the maximum sunshine hour's is approximately 3000 hr/year (Alasady, 2011). Iraqi climate is characterised by a hot and long summer season where the ambient temperature can reach 50 °C; consequently, air-conditioning systems are essential in the buildings. Istepanian (2014) showed that in 2015 the demand for electricity in the residential sector will reach 80% of the total electrical energy demand in Iraq, and he also predicted that this demand will maintain approximately the same level until 2030. Abdulsada & Salih (2015) reported that 60% of the electricity supplied to the residential buildings is consumed by air conditioning systems. Thus, in order to reduce this electricity consumption, cooling systems that using alternative energies, such as solar energy, would be the best choice.

The literature is abundant with comprehensive reviews of solar adsorption systems, (Fernandes et al., 2014; Hassan & Mohamad, 2012; Wang, Wang & Oliveira, 2009; Wang, Wang & Wu, 2014; White, 2013), however, there is still a significant amount of research needed to make the solar adsorption system more comparable with traditional cooling systems through enhancement of the performance of the system and developing new designs with low costs.

1.3 Aim and objectives of the research

The performance of a solar cooling system depends on its specification and the sizes of its components as well as on the climate conditions and building type. The main aim of this study is to design the most feasible solar adsorption system for a domestic building under Iraqi climate conditions. In order to achieve this aim, the following objectives were defined:

- A review of solar adsorption technology and a full description for the system.
- Develop the system using the Transient System Simulation program (TRNSYS) coupled to the MATLAB software.
- Parametric study of the solar adsorption system through energy, exergy and economic analysis.
- Develop a multi-objective optimisation solution in order to optimise the solar adsorption system on an exergy efficiency and economic basis.

To achieve the research objectives, this thesis focuses on system design, model development, system simulation and development of an optimum solar adsorption system.

Figure 1-3 illustrates the approach adopted for this research.

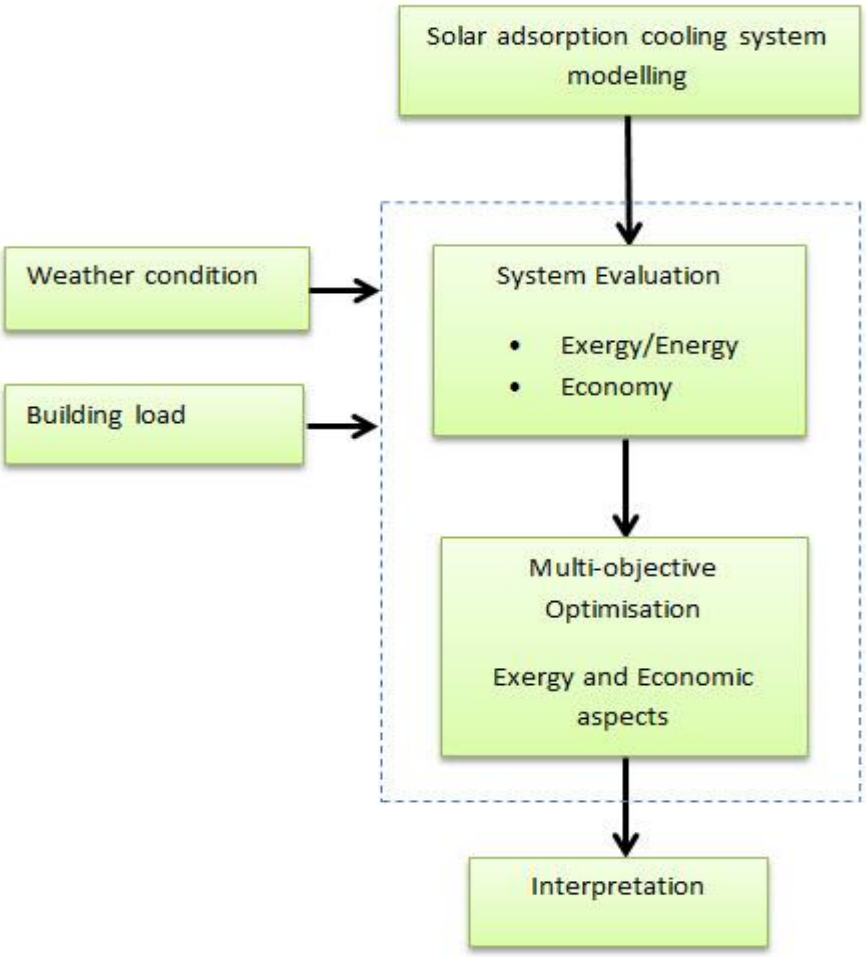

Figure 1-3 Flow chart of research approach.

1.4 Contributions of this Research

This research is considered to be the first study that deals with a solar adsorption air conditioning system under Iraqi climate conditions for domestic applications, and with the optimisation of the design through a multi-objective genetic algorithm technique.

1.5 Outlines of Thesis

An introduction to solar energy and solar cooling systems has been explained in Chapter One. A description of the components of the solar adsorption system is presented in Chapter Two, followed by modelling of the system in TRNSYS software in Chapter Three. Energy, exergy and economic analyses are made clear in Chapter Four. Chapter Five presents the parametric study results, where the performance of the system is assessed on the bases of exergic and

economic aspects. In Chapter Six, a multi-objective optimisation problem is developed. Best solutions are demonstrated by implementing the genetic algorithm (GA) optimisation technique. A process of decision-making is used to find the optimum solution, and the payback period of the system has been estimated. In Chapter Seven, the conclusions from the study and future work recommendations are summarised.

Chapter Two

System Design and Description

2.1 Introduction

A solar adsorption cooling system uses solar energy as the primary resource to provide a cooling effect for a building. It works by using solar collectors to collect solar energy and converting it into thermal energy in the form of heat transfer fluids circulating through the system. Since solar energy is not continuously obtainable, a solar adsorption cooling system needs to be connected with an auxiliary heater and thermal energy storage tanks in order to increase its performance. Figure 2-1 shows a schematic diagram of the solar adsorption cooling system investigated in this research. Hot Water flows from the Hot Storage Tank to the Auxiliary Heater (to offset the temperature of the fluid if it falls below the set temperature of 85°C).

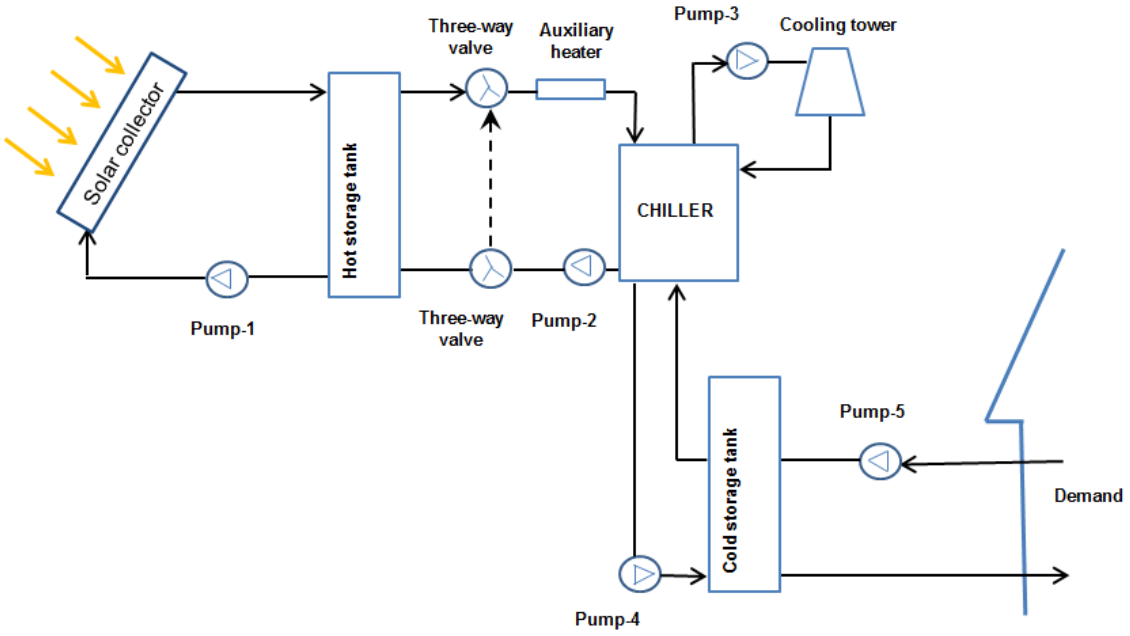

Figure 2-1 Schematic of a solar adsorption cooling system.

It then enters the Adsorption Chiller to complete a desorption process in the first bed, while a Cooling Tower is connected to the chiller in order to reduce the fluid temperature when it exceeds 27°C. Cold water enters the chiller to complete the adsorption process in the second bed, and in turn produces Chilled Water for cooling demand via a cold storage tank.

The solar adsorption chiller system usually consists of three main loops (Hot Water Loop, Cooling Water Loop, and Chilled Water Loop) as shown in the above diagram.

2.2 Working pairs (Adsorbent & Adsorbate)

The working pairs of an adsorption chiller are made up of adsorbent (solid) and adsorbate (refrigerant). The adsorbent materials can be generally divided into two types: the physical adsorbents, such as Zeolite, Silica gel, activated carbon and activated carbon fibre, and the chemical adsorbents, such as metal chlorides, metal oxides and metal hydrides (Wang, Wang & Oliveira, 2009). Table 2-1 shows the required properties of adsorbent and adsorbate materials.

Table 2-1 Desired properties of the adsorbent and adsorbate materials (Ozgen, 2008; Şasmaz, 2011; Wang et al., 2009).

Adsorbent	Adsorbate
High ability to adsorb the adsorbate – high adsorption capacity and easily regenerated	Evaporation temperature below zero degrees, such as ammonia
Low specific heat	High latent heat and a suitable boiling point
Good thermal conductivity	Non –toxic, non –flammable and non-corrosive
It is non-corrosive	High thermal conductivity
It is non-toxic	Low viscosity
It has chemical and physical stability	Low saturation pressure
Low cost and widely available	Environmental harmless

Alam et al. (2000) observed that the most popular adsorbents are Zeolite, Silica gel and activated carbon. For air conditioning applications, Anyanwu & Ogueke (2005) found that zeolite-water is “the best pair”. Fernandes et al. (2014) also stressed that the Zeolite-water working pair (Zeolite as adsorbent and water as adsorbate) is more suitable than the Silica-gel pair for air conditioning applications. However, Wang *et al.* (2009) stated that the silica gel-water is “attractive to be used in a solar cooling system” because it needs low driven heat temperatures (less than 90°C). Nevertheless, Ozgen (2008) showed that the zeolite-water pair is better than the silica gel-water pair for the 80°C-100°C range. This range of the temperature can be obtained by using an evacuated tube collector (which will be explained in the next section).

2.3 Adsorption Chiller

In general, solar adsorption cooling systems are divided into two types; first, basic adsorption cycle which the bed is integrated with the solar collector. This type works intermittently where the desorption process occurs during the day and the cooling effect is achieved only at night time. This kind of adsorption system is used for ice production only. Second, the heat recovery cycle, in which the adsorber bed is separated from the collector and a two-bed (or multi-bed) is used to obtain a continuous cooling effect (Yong & Sumathy, 2004). In the present study a two-bed adsorption chiller is used; more information about multi beds can be found in Hassan & Mohamad (2012). Each bed is connected with the condenser and the evaporator, and all these components are in the same chamber. As shown in Figure 2-2, there are four basic stages in the solar adsorption refrigeration working principles:-

i) 1-2 Isosteric heating [heat added to the bed (pre-heating)].

ii) 2-3 Isobaric heating [desorption process].

iii) 3-4 Isosteric cooling [coolness added to the bed (pre-cooling)].

iv) 4-1 Isobaric cooling [adsorption process].

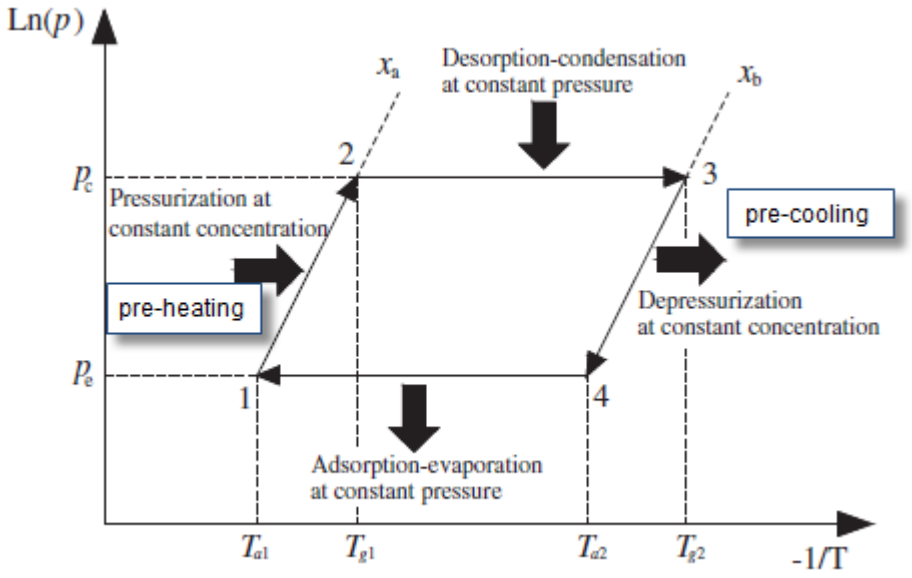

Figure 2-2 Clapeyron (p-T-x) diagram for the ideal adsorption refrigeration cycle (Wu, Zhang & Men, 2011).

A scheme of a two bed adsorption chiller unit is shown in Figure 2-3. The Adsorption Chiller unit consists of two beds (Bed 1 and Bed 2), one Condenser and one Evaporator. There are four modes (Modes A, B, C and D), in the operating cycle of the system.

- In Mode A, only the valves (V1, V3) are opened; in this case the Evaporator and Bed 1 are in the adsorption process and the condenser is connected with Bed 2. Due to the low pressure of the refrigerant in the Evaporator, it starts to evaporate and then the adsorption water vapour is adsorbed on the surface of the solid adsorbent (Zeolite) in Bed 1, and the cooling water removes the adsorption heat; this is known as the adsorption process. The result from this adsorption process in the Evaporator is that the refrigerant evaporates and generates cooling, which can be used for air-conditioning. Meanwhile, the Condenser and Bed 2 are in a desorption process, where the refrigerant is desorbed from the adsorbent by heating in Bed 2, and then flows to the Condenser to be liquefied, using cooling water to remove the latent heat, while the condensate refrigerant is returned to the Evaporator through a U-bend tube, which is used to keep the pressure between the Condenser and Evaporator at different levels. These two processes continue until the system reaches a near equilibrium level,
- The cycle will be switched for in a short duration to Mode B, which is known as pre-heating and pre-cooling of Bed 1 and Bed 2, respectively. In this mode all four valves are closed until the pressure of Bed 1 (desorber) and Bed 2 (adsorber) are nearly equal to the Condenser and Evaporator pressure.
- In Mode C, the valves V2 and V4 are opened to connect Bed 1 with the Condenser to be in the desorption process, and Bed 2 with the Evaporator to be in the adsorption process. Mode C is exactly the opposite of Mode A and
- Mode D is exactly the opposite of Mode B, where pre-cooling of Bed 1 and pre-heating of Bed 2 occurs in this mode. After Mode D, the adsorption chiller returns to Mode A, hence a complete system cycle is defined (El-Sharkawy, AbdelMeguid & Saha, 2013; Saha et al., 2007).

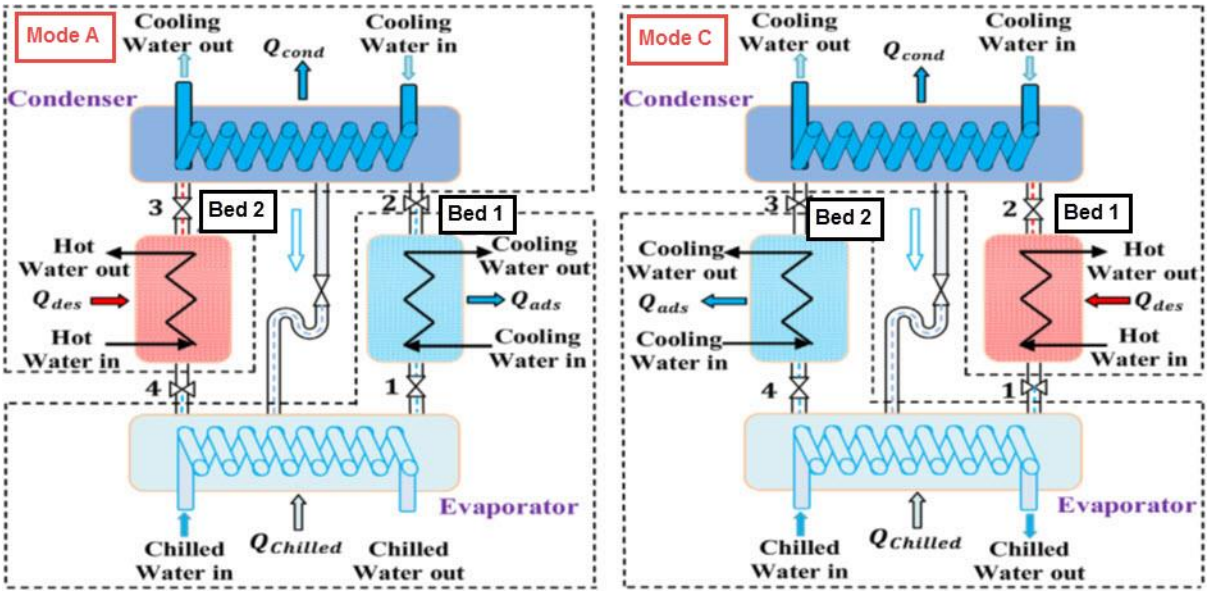

Figure 2-3 A schematic diagram of an adsorption chiller unit (Sadeghlu et al., 2014).

2.4 Hot Water Loop

The Hot Water loop can be divided into two loops due to thermal stratification for the Hot Storage Tank and an Auxiliary Heater. On the hot side of the tank, the collector generates hot water and then stores it in the tank. Meanwhile, on the load side of the tank, the tank is connected with the auxiliary heater, which will be used when needed, in order to achieve the hot water design and operating inlet temperature to the chiller through additional heating. Figure 2-4 shows the scheme of the Hot Water loop.

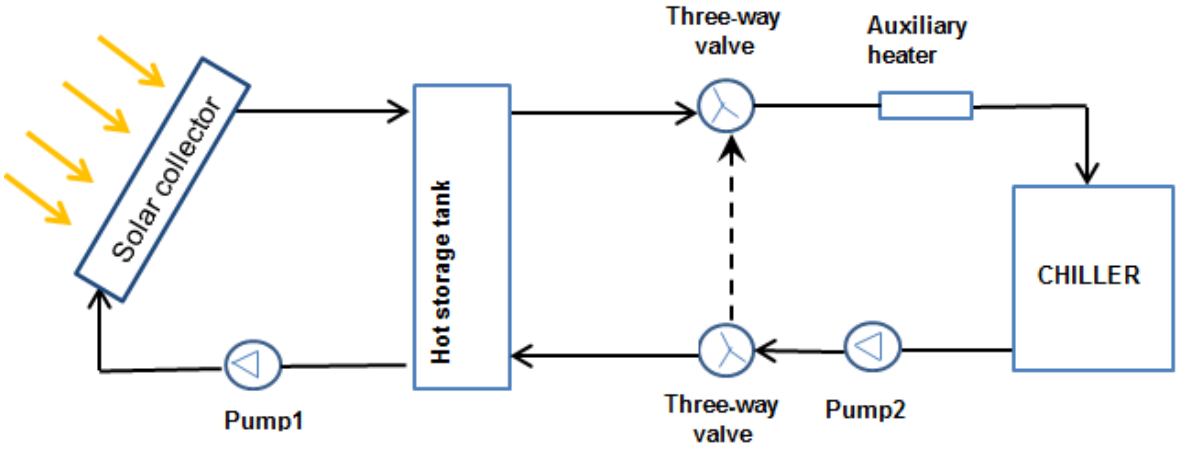

Figure 2-4 Scheme of the hot water loop.

The returned water from the chiller is diverted by using a three-way valve. If the temperature of the water is higher than the storage water temperature, it returns to the auxiliary heater directly and bypasses the storage tank. However, if the hot side tank temperature is greater than the returned water temperature, it will flow to the tank in order to attempt to reach the set point temperature (hot water design inlet temperature of the chiller).

2.4.1 Solar Collectors

> "Solar energy collectors are special kind of heat exchangers that transform solar radiation energy to internal energy of the transport medium." (Kalogirou, 2004).

The solar collector transfers the sun's radiation to heat by absorbing sunlight, and stores it as useful thermal energy in the heat transfer fluid.

Basically there are two types of solar collectors:

i) Non-concentration (stationary): such as
   1. Flat plate collectors (FPC).
   2. Evacuated tube collectors (ETC).
   3. Compound parabolic collectors (CPC).

ii) Concentrating (absorbing and reflecting absorbing): such as
   1. Parabolic through collectors.
   2. Linier Fresnel reflectors.
   3. Parabolic dish reflectors.
   4. Heliostat field collectors.
   5. ICS collectors.
   6. Air collectors.
   7. Pool collectors.

Table 2-2 Typical concentration ratio and temperature range of each type of collector (Kalogirou, 2004).

Motion	Collector type	Absorber shape	Concentration ratio *	Temperature range(C^0)
Stationary	Flat Plate Collector (FPC)	Flat	1	30-80
	Evacuated Tube Collector(ETC)	Flat	1	50-200
	Compound Parabolic Collector(CPC	Tubular	1-5	60-200
Single-axis tracking			5-15	80-300
	Linear Fresnel Reflector (LFR)	Tubular	10-40	80-250
	Parabolic Trough Collector (PTC)	Tubular	15–45	60–300
	Cylindrical Trough Collector(CTC)	Tubular	10-50	80-300

Two-axis tracking	Parabolic Dish Reflector (PDR)	Point	100-1000	100-500
	Heliostat Field Collector (HFC)	Point	100-1500	150-2000

* Concentration ratio is ratio of amount of light energy to the collector area

The evacuated tube collector is an improved form of flat plate collector. Morrison et al. (2004) showed that the evacuated tube solar collector has better performance than flat plate collectors especially in high temperature processes (50-200 ^{0}C). Moreover, the "Satisfactory performance, reliability and cost-effectiveness" of the evacuated tube solar collector make it more attractive among the stationary collectors (Milani & Abbas, 2016). Therefore, in this study the evacuated tube collector (ETC) is selected.

The evacuated tube collector is commercially obtainable in two different designs:

a) Direct flow collector.
b) Heat pipe collector.

The heat pipe type evacuated tube solar collector is selected for our system because of the higher temperature range and the simplicity of the arrangement. Figure 2-5 shows the heat pipe evacuated tube collector with a cylindrical absorber.

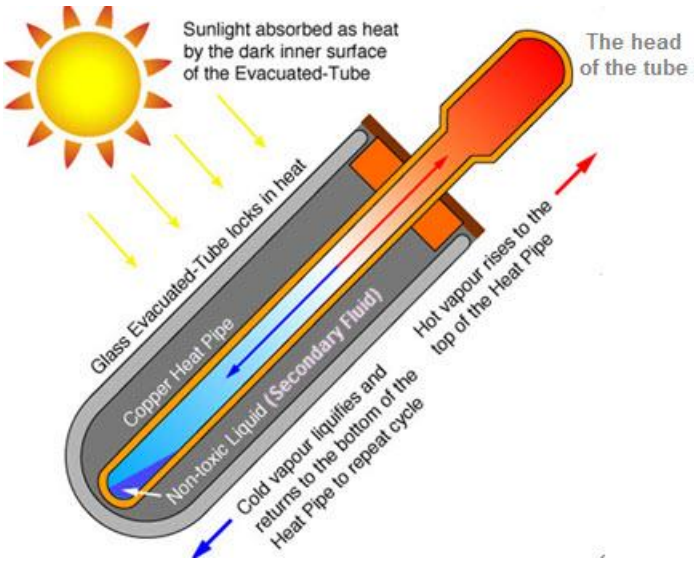

Figure 2-5 Schemed diagram of heat pipe evacuated tube solar collector (Jakobe, 2014)

In this type of solar collector there is no fluid stream through the evacuated tube. Instead, there is a secondary fluid (non-toxic liquid) which is used to transfer the heat from the top of the evacuated tube to the system fluid, through a recirculating mechanism of evaporation and condensation inside the heat pipe. The secondary fluid evaporates to vapour and rises to the top of the heat pipe by absorbing solar radiation from the absorber. At the top of the head of

the tube, the vapour condenses and releases the thermal energy which was taken earlier; and flows back to the bottom of the tube to be evaporated once more.

2.4.2 Hot Storage Tank

The hot water storage tank is used to store the energy between the collector and the chiller in order to increase the efficiency of the system (Li & Sumathy, 2001). There are two technologies for hot storage tanks, the multi-nodes method (with thermal stratification) and the plug flow method (without stratification). In this study a thermal stratification storage tank has been used. In this type the tank is divided into several sections (*N* nodes); each node is assumed to be isothermal and reacts with the nodes above and below, depending on the inlet fluid temperature. For example, in the tank with five nodes as shown in Figure 2-6, the hot water from the collector enters the top of the tank at (T_{co}) and flows to the node which has the same density. If $T_{s3} < T_{co} < T_{s2}$, in this case the water will be distributed among nodes 1, 2 and 3 (Dincer & Rosen, 2011), as shown.

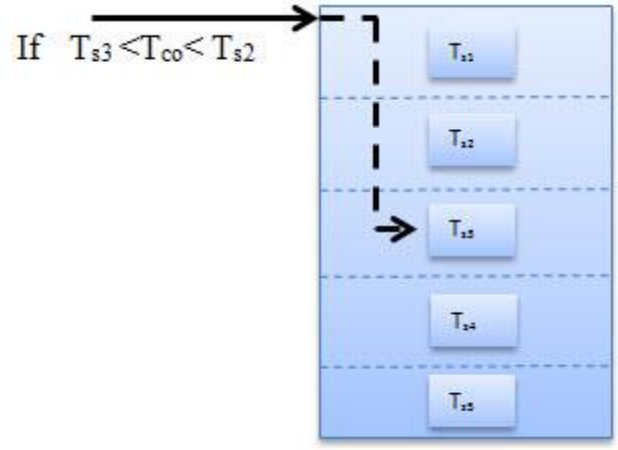

Figure 2-6 Stratification storage tank concepts

2.4.3 Auxiliary Heater

A back-up heating system is intermittently employed in solar cooling systems. When there is not enough solar radiation, it is important to be sure that the temperature of the fluid which enters the chiller will not fall below the set point temperature. Consequently, the auxiliary heater will prevent this drop in the temperature, and control it by heating up the fluid in order to maintain it at a desired temperature level (Duffie & Beckman, 1980).

2.5 Cooling Water Loop (heat reject sub-system)

A cooling tower is used to reject unwanted heat from the chiller to the ambient air. Figure 2-7 shows a scheme for the cooling water loop. There are two types of cooling tower, wet cooling tower (direct contact) and dry cooling tower (indirect contact). The working fluid in the dry cooling tower is separated from the ambient air and the process water, while in the wet cooling tower the warm water stream is in directly contact with the air (at ambient temperature). In the present study a wet cooling tower has been chosen to cool the water stream and keep it below the set point temperature of cooling water in the chiller. The water will be cold due to the temperature difference between the air and the water and also because of mass transfer (resulting from evaporation) to the air. This process depends on the relative humidity of the air, wind velocity, specific mass flow rate of the fluid, and the air also depends on the inlet temperature of the water to the cooling tower (Fisenko, Brin & Petruchik, 2004).

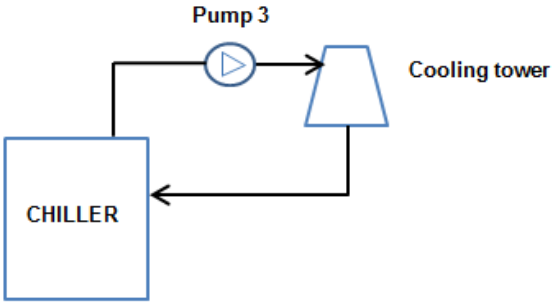

Figure 2-7 Scheme for the cooling water loop

2.6 Chilled Water Loop

The chilled water produced from the adsorption chiller, which is stored in a cold storage tank (similar to the hot storage tank), is used to accumulate excess chilled water for use later when required. Figure 2-8 shows a scheme for the chilled water loop.

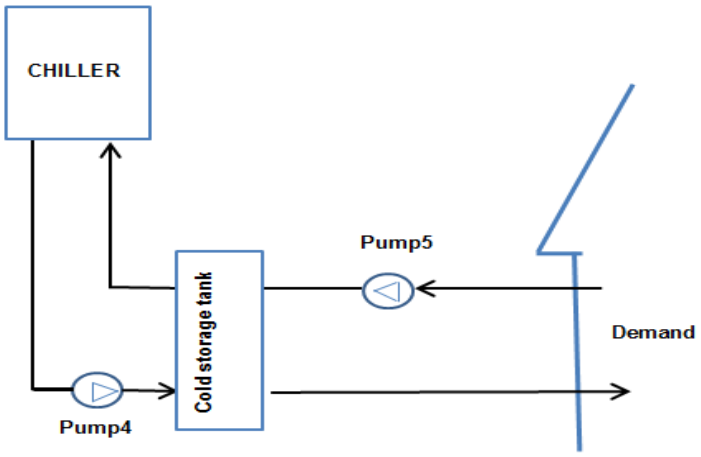

Figure 2-8 Scheme for the chilled water loop

The use of a storage tank has many advantages, such as: it decreases the energy consumption, offers flexibility of system operation. Moreover, it is especially important in a country with a hot climate because it improves the indoor air condition on demand (Dincer & Rosen, 2001).

2.7 Summary

This second chapter has described an overview of the system in general. All the components of the system were defined and each component explained separately. The adsorption chiller was described first because it is a central point in the system. In addition, the fluid flow path in the system was defined by describing all three loops, hot water loop including (solar collector, hot storage tank and auxiliary heater), cooling water loop which is considered as a heat reject sub-system and known as cooling tower, and finally chilled water loop which contains the cold storage tank.

Chapter Three

System modelling

3.1 TRNSYS

The solar adsorption cooling system was modelled using the TRNSYS simulation programme (Transient System Simulation). TRNSYS is an extremely flexible, graphical interface based software environment to simulate the dynamic behaviour of transient systems and solve problems of modelling and analysing the performance of complex energy systems, such as thermal, electrical and integrated energy systems ('TRNSYS,').

The main interface of TRNSYS software is the ‘Simulation Studio’, which can be used to build a TRNSYS project by adding and connecting the components in the working area. Each project consists of many interconnected individual components. Each component is known as a ‘unit’ and every unit in a system is described by a ‘Type’ (For example, Type 71 is an evacuated tube collector). By connecting these Types with one another, a model (integrated energy system) can be built. Moreover, each Type in the simulation studio has a set of matching requirements known as ‘Performa’ which describes the parameters, input, output and external files of the component (Klein, Beckman & Mitchell, 2014b).

3.2 System Overview

The adsorption cooling system developed in TRNSYS includes three loops:-

- Hot water loop [used to harvest the solar energy and store it in the hot storage tank, with the auxiliary heater for additional heating].
- Cooling water loop [used to reject the waste heat from the system].
- Chilled water loop (the Load Loop) [used to deliver the chilled water to the demand side].

The type of adsorption chiller is the central point that connects the three loops which will be further discussed in Section 3.3.4. Figure 3-1 shows the schematic of the solar adsorption cooling system. Solar radiation is absorbed by the evacuated tube solar collector to heat up the mixture of water coming from (1) and water flows from the collector to the top of the hot

storage tank (2). The warm water returns from the bottom of the tank (1') to the collector to be heated up again. The second part of the storage tank from the top (4) supplies the hot stream to the adsorption chiller (6). The hot water, before entering the chiller, passes through an auxiliary heater (5) which is used to maintain the temperature of the water stream if necessary. The adsorption chiller produces the chilled water (11) which is stored in the cold storage tank (11'). The chilled water after storage is accessed by the cooling demand (12). The cooling water loop is used to remove the excess heat from the chiller (9) by a cooling tower which cools down the water (8) and supplies it back to the chiller once more.

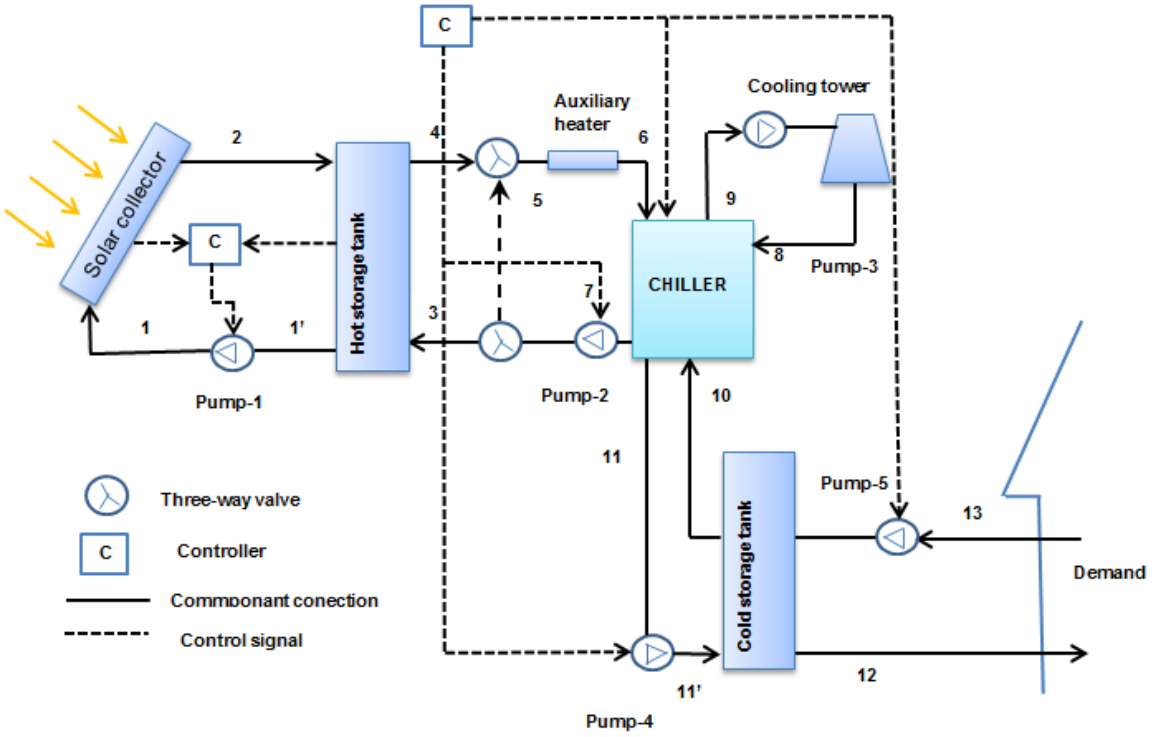

Figure 3-1 Schematic of solar adsorption cooling system

3.3 TRNSYS Components

The schematic diagram of the solar adsorption system in TRNSYS is shown in Figure 3-2. The system is modelled by inputting the different components into the simulation studio of the TRNSYS software. The components of the hot water loop are connected by thick red lines, whereas the chilled water loop is represented by the thick purple lines; and those connected by thick blue lines represent the cooling water loop of the chiller. Further details of each component will be discussed in the following sections.

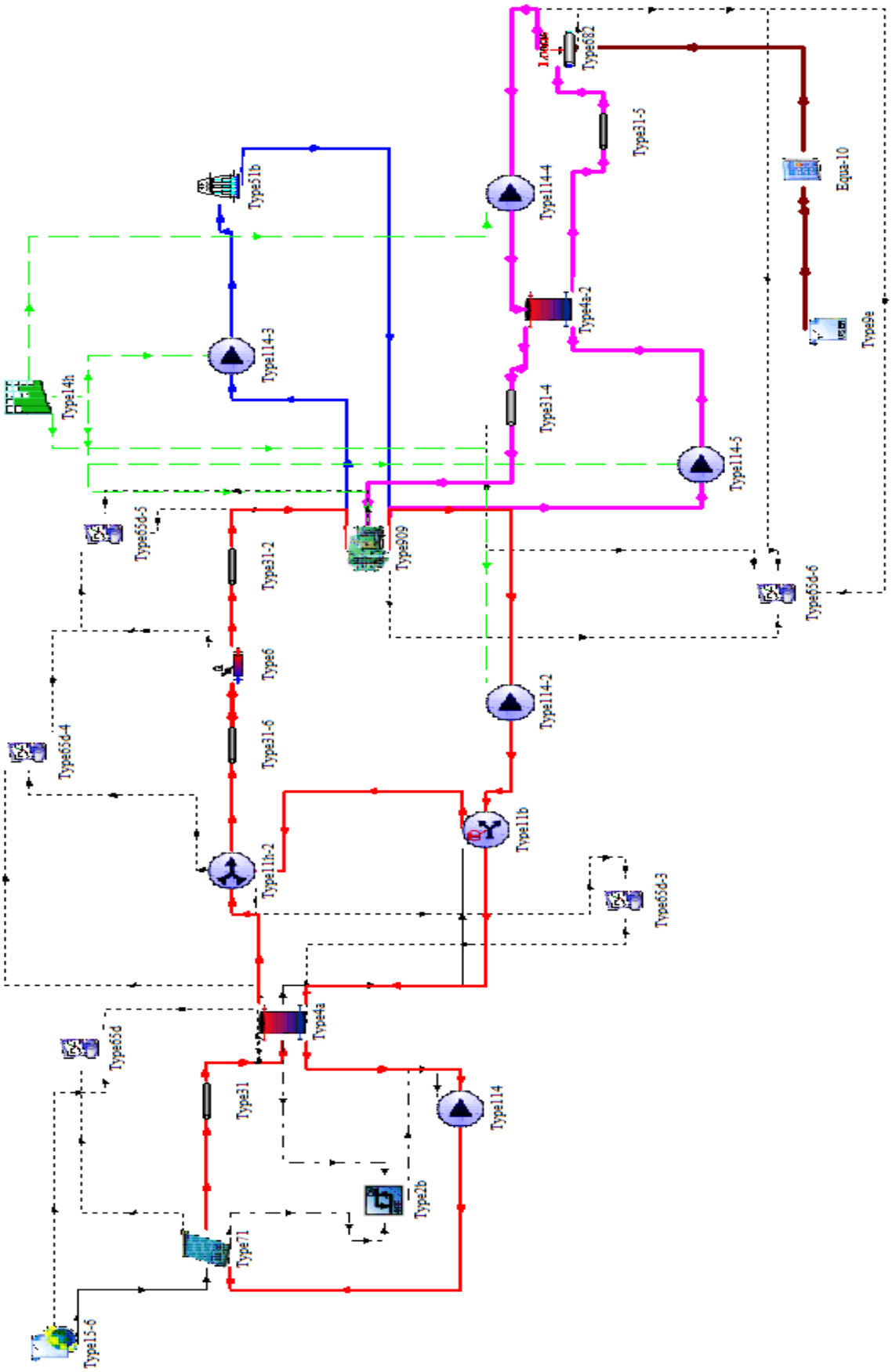

Figure 3-2 TRNSYS scheme of the solar adsorption system

3.3.1 Type 71 - Evacuated Tube Solar Collector

The evacuated tube solar collector (Type 71) was selected from the TRNSYS component library to model the collector. The evacuated tube solar collector transfers solar energy to thermal energy and heats up the water. The thermal performance of the collector is determined by using a text file that includes a list of data of longitudinal and transverse incidence angle modifiers (IAM). The collector thermal efficiency of an evacuated tube solar collector can be obtained by using Equation 3-1 (Klein, Beckman & Mitchell, 2014b)**.**

$$\eta = a_o + a_1 \frac{\Delta T}{I_T} - a_2 \frac{(\Delta T)^2}{I_T} \qquad \text{Equation 3-1}$$

Where:-

(a_o) is the optical efficiency.

(a_1) is the first order coefficient.

(a_2) is the second order coefficient.

(ΔT) is temperature difference between inlet temperature of the collector and the ambient temperature.

(I_T) is total incidence of solar radiation.

The thermal efficiency, as defined by 3 parameters: a_0, a_1 and a_2, are shown in Table 3-1 according to published test results by Apricus Solar Company (Davis, 2014).

Table 3-1 Collector input parameters.

Name	Value	Unit
Fluid Specific Heat	4.19	kJ/kg.K
Specified Flow rate /unit area	72	kg/hr.m²
Optical efficiency (a_0)	0.71	-
First order IAM (a_1)	1.737	W/m².K
Second order IAM (a_2)	0.008	W/m².K

3.3.2 **Type 4a - Thermal energy storage model**

A stratified storage tank is modelled by Type 4a in TRNSYS software. The thermal performance of the tank can be modelled by supposing that the tank consists of N (N≤100) nodes of full-mixed and equal volumes, as shown in Figure 3-3. A fluid-filled sensible energy storage tank is divided in to a number of nodes, and each node is isothermal and reacts with the node above and below in several mechanisms, such as the movement and conductivity of the fluid. If the number of the nodes is one, the tank will be a fully-mixed tank, and if it is more than one node, the top of the tank will be hotter than the bottom. In the present study, the number of nodes used is 5 for both the hot storage tank and the cold storage tank. The overall tank loss coefficient (average tank loss coefficient to the surrounding per unit area) is assumed to be 0.75 W/m².K for the hot storage tank and 0.5W/m^2.K for the cold storage tank (Januševičius, Streckienė & Misevičiūtė, 2015)

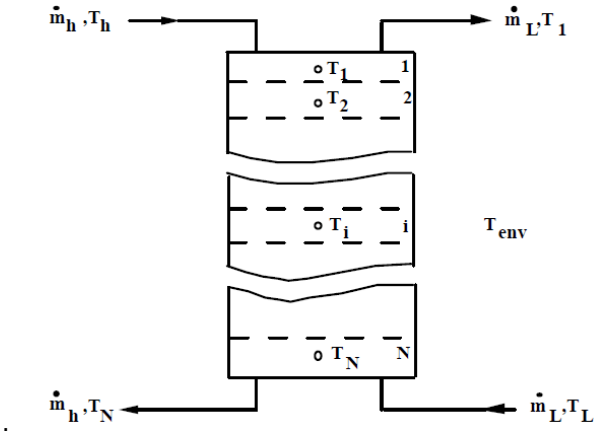

Figure 3-3 Stratified storage tank (Klein, Beckman & Mitchell, 2014a)

Assuming that at each node the fluid stream flowing up and down is fully mixed before entering each segment, Figure 3-4 shows the *i*th segment of the tank and the flow streams will be (m_1), (m_2) (m_3) and (m_4) as water flows up or down (Klein, Beckman & Mitchell, 2014b). The energy balance on the segment is:

$$m_i Cp_f \frac{dT_i}{dt} = \begin{cases} \dot{m}_1 - \dot{m}_3 Cp\left(T_{i-1} - T_i\right) & \dot{m}_1 \geq \dot{m}_3 \\ \dot{m}_3 - \dot{m}_1 Cp\left(T_{i+1} - T_i\right) & \dot{m}_1 < \dot{m}_3 \end{cases} \qquad \text{Equation 3-2}$$

Where:-

(m_i) is mass of the fluid in the segment.

(Cp_f) is specific heat of the fluid.

(T_i) is the temperature of the tank segment.

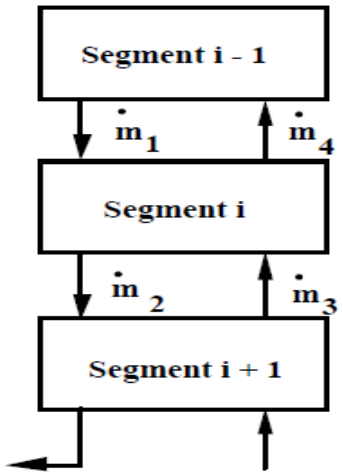

Figure 3-4 The flow stream between the segments (Klein, Beckman & Mitchell, 2014a)

3.3.3 Type 6 - Auxiliary heater

The auxiliary heater is modelled by Type 6. The main reason for using the auxiliary heater is to raise the temperature of the flow stream when it decreases below the set point, in cases when the solar energy is not available or insufficient, and the storage energy in the tank has been depleted. The auxiliary heater works as an external (on/off) heating device. The energy balance for the auxiliary heater is shown in Figure 3-5, where (T_{am}) is the ambient temperature, (T_{av}) is average temperature of the fluid.

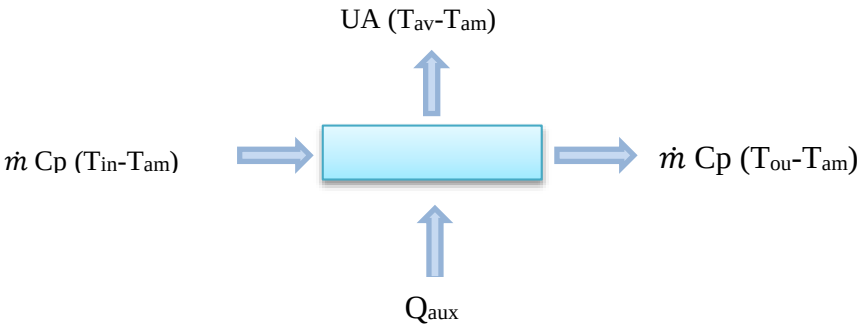

Figure 3-5 The energy balance of auxiliary heater

From the energy balance equation, the outlet temperature can be calculated by Equation 3-3 (Klein, Beckman & Mitchell, 2014b) .

$$T_{out} = \frac{\dot{m} Cp T_{in} - UA\left(\frac{T_{in}}{2}\right) + UAT_{am} + \dot{Q}_{\max}\eta_{aux}}{\dot{m} Cp + \left(\frac{UA}{2}\right)} \qquad \text{Equation 3-3}$$

Where:-

(U) is the heat transfer coefficient.

(A) is the area.

(T_{am}) is the ambient temperature.

(η_{aux}) is auxiliary heater efficiency.

The model can also be used to calculate the heater losses to the ambient air with the following equations:-

$$\dot{Q}_{loss} = UA(T_{av} - T_{am}) + (1 - \eta_{aux})\dot{Q}_{\max} \qquad \text{Equation 3-4}$$

Where the average temperature is:-

$$T_{avg} = \frac{(T_{out} - T_{in})}{2} \qquad at\ T_{in} \geq T_{set}.$$

$$T_{avg} = \frac{(T_{set} - T_{in})}{2} \qquad at\ T_{out} > T_{set}.$$

The auxiliary energy transferred from the heater to the fluid to the water can be calculated by Equation 3-5.

$$\dot{Q}_{aux} = \frac{\dot{m} Cp(T_{set} - T_{in}) + UA(T_{avg} - T_{am})}{\eta_{aux}} \qquad \text{Equation 3-5}$$

In this study the heating capacity of the auxiliary heater is 34.6 kW (according to the data sheet of the chiller (InvenSor, 2013)) and the set point of the temperature is set to 85^0C.

3.3.4 **Type 909 - Adsorption chiller**

Type 909 is used to model the adsorption chiller, which will depend on an external data file. The data file provides values of normalized chiller's capacity and normalized Coefficient of Performance (COP) ratio as a function of hot water inlet temperature, cooling water temperature and chilled water temperature. The first calculation performed by Type 909 is to calculate the chilled water energy by applying Equation 3-6 (Thornton, Bradley & McDowell, 2014).

$$Q^{\bullet}_{chill} = \min\left(Q^{\bullet}_{capacity}\right)$$

Or

$$\dot{Q}_{chill} = \min\left(\dot{m}_w Cp_w\left(T_{chill,in} - T_{chill,set}\right)\right) \qquad \text{Equation 3-6}$$

Where:-

$\left(T_{chill,set}\right)$ is the set point temperature of the chilled water outlet in K.

$\left(\dot{m}_w\right)$ is mass flow rate of the chilled water in kg/hr.

$\left(Cp_w\right)$ is the heat capacity of the chilled water in kJ/kg.K.

$\left(\min\right)$ is the minimum.

The outlet of the chilled water stream is calculated as:-

$$T_{chill,out} = T_{chill,in} - \left(\frac{\dot{Q}_{chill}}{\dot{m}_w Cp_w}\right) \qquad \text{Equation 3-7}$$

The hot water energy required to regenerate the chiller is:-

$$\dot{Q}_{hot,w} = \frac{\dot{Q}_{chill}}{COP} \qquad \text{Equation 3-8}$$

And the amount of heat rejected from the chiller can be expressed as a summation of the chilled water energy plus hot water and auxiliary heater energy:-

$$\dot{Q}_{heat,rejection} = \dot{Q}_{chill} + \dot{Q}_{hot,w} + \dot{Q}_{aux}$$ Equation 3-9

Equations 3-6 to 3-9 provide the mathematical model for the adsorption chiller Type 909. The model selected in this study is the InvenSor HTC18 plus, and Table 3-2 shows the specification for this adsorption chiller.

Table 3-2 Specifications of the InvenSor HTC18 plus adsorption chiller (InvenSor, 2013).

Chiller model :InvenSor HTC 18 plus			
Cooling Capacity		18	kW
Rated COP		0.52	-
Heat water	Inlet temperature	85	^{o}C
	Outlet temperature	76.5	^{o}C
	Temperature range	75-100	^{o}C
	Volume flows	3600	L/hr
Cooling water	Inlet temperature	27	^{o}C
	Outlet temperature	34.5	^{o}C
	Temperature range	20-47	^{o}C
	Volume flows	6000	L/hr
Chilled water	Inlet temperature	18	^{o}C
	Outlet temperature	14	^{o}C
	Temperature range	9-25	^{o}C
	Volume flows	3900	L/hr

3.3.5 Type 51b - Cooling Tower

The cooling tower is modelled by using Type 51b. The warm water from the chiller is pumped to the top of the tower and sprayed down, and the ambient air is drawn upward (direct contact type). The water stream is cooled as a result of sensible and latent heat transfer because of the temperature differences between the ambient air and the warm water. The schematic of a counter flow forced-draft cooling tower is shown in Figure 3-6. The cooling tower consists of several cells usually arranged in parallel. The losses of the water through the cell can be replaced by the make-up water.

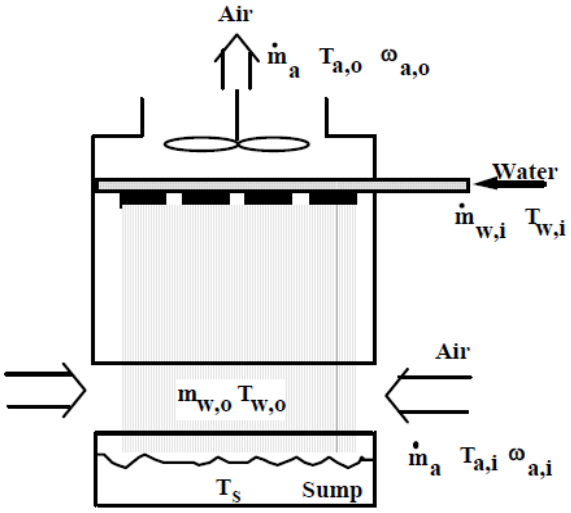

Figure 3-6 Schematic of a single cell cooling tower (Klein, Beckman & Mitchell, 2014b)

The air inlet condition to the tower is known and can be characterised by the temperature, mass and humidity ratio; whereas the inlet of the water is characterised by the mass flow rate and the temperature. The amount of heat removed by the cooling tower can be calculated from Equation 3-10 (Klein, Beckman & Mitchell, 2014b):-

$$\dot{Q}_{cell} = \upsilon_{air}\,\dot{m}_{air}\left(h_{a,w,in} - h_{a,in}\right) \qquad \text{Equation 3-10}$$

Where:-

(υ_{air}) is air-side heat transfer effectiveness.

$(h_{a,w,in})$ is inlet enthalpy of moist air per mass of dry air at water inlet temperature.

$(h_{a,in})$ is inlet enthalpy of moist air per mass of dry air.

In the model there are two modes: the user can use either the coefficients of the mass transfer correlation or an external data file. The coefficients of the mass transfer correlation, c and n, taken in this study were 0.5 and -0.85 respectively (Martínez, Martínez & Lucas, 2012). The cooling tower model is TEVA TVA008.

In addition to these key components above, there are secondary components used in the model such as pumps (solar circuit (0.43 kW), chilling circuit (0.29 kW), recoiling circuit (0.57 kW), and drive circuit (0.27 kW)) and pipes.

3.3.6 Control strategies

There are three controllers used in the system, first to control the flow through the collector, second to control the hot water outlet from the chiller, third to control the time operation of whole system. The functioning of these controllers is as follows:-

- **Type 2b - Collector control**

The stream flow through the collector needs to be controlled in order to maintain the temperature of the outlet collector below 100 °C, and also to reduce energy loss of the fluid to the surroundings. Type 2b is used to control the flow through the collector, since the pump is at a fixed speed so the flow can either be the rated flow or zero. This controller provides a control signal to the solar collector pump, after determining whether the pump should be switched OFF or ON. The controller activates and deactivates the solar pump in two conditions: (1) when the outlet temperature of the collector is greater than the bottom storage tank temperature by more than 5 °C, and (2) the controller deactivates the pump when the temperature difference is less than 2 °C.

- **Type 11b - Chiller return Three-way valve**

The three-way valve is modelled by using Type 11b in order to control the return water stream from the chiller. If the returning water temperature from the chiller is higher than the storage hot water temperature, the returning flow bypasses the hot storage tank and is sent directly back to the auxiliary heater.

- **Type 14h - Forcing Function**

Type 14h is used to control the whole cycle time operation from 8:00 to 18:00 hours. It serves as a master control for all components except the pump of the collector. Accordingly, it shuts off the components after the working hours, irrespective of their individual control signals.

3.3.7 Type 15-6 -Weather data

Type 15-6 is a data file which can calculate total, beam, and sky diffuse solar irradiance, the angle of incidence of beam solar radiation, ground reflected solar radiation and the slope and azimuth angles. The Type further includes evaluation of mains water temperature and effective sky temperature for radiation calculations. The weather data used in this study is typical meteorological year TMY2 (which is a collation of selected metrological elements

data taken from a data bank to represent the typical weather phenomena of the site) for Baghdad city that is available in TRNSYS software.

3.4 Sample of preliminary results of the system model by TRNSYS software

The first result of the simulation after completing the modelling on TRNSES software is shown in Figure 3-7, where the model was simulated from April (hour 2160) to the end of October (hour 7296). The values of the temperatures produced from the chiller and the amount of solar fraction are illustrated in the figure. It is obvious that the chilled water is in the range 12-14 ^{0}C, the cooling water temperature is in the range 32-34 ^{0}C and the hot water is 76-79 ^{0}C. These values are similar to the parameters of the InvenSor HTC 18 plus adsorption chiller as shown in Table 3-2. A key criterion describing the energy performance of the system is known as the solar fraction (*SF*), which can be defined as the ratio of the thermal energy produced by the collector to the total energy, and can be expressed as (Baniyounes *et al.*, 2013):-

$$SF = \frac{Q_{sol}}{Q_{sol} + Q_{aux}} \qquad \text{Equation 3-11}$$

Where:-

(Q_{sol}) is the useful energy gain of the evacuated tube collectors.

(Q_{aux}) is the energy of auxiliary heater.

The influence of changing the parameters of the system on the amount of the solar fraction will be presented in the parametric study (Chapter 5).

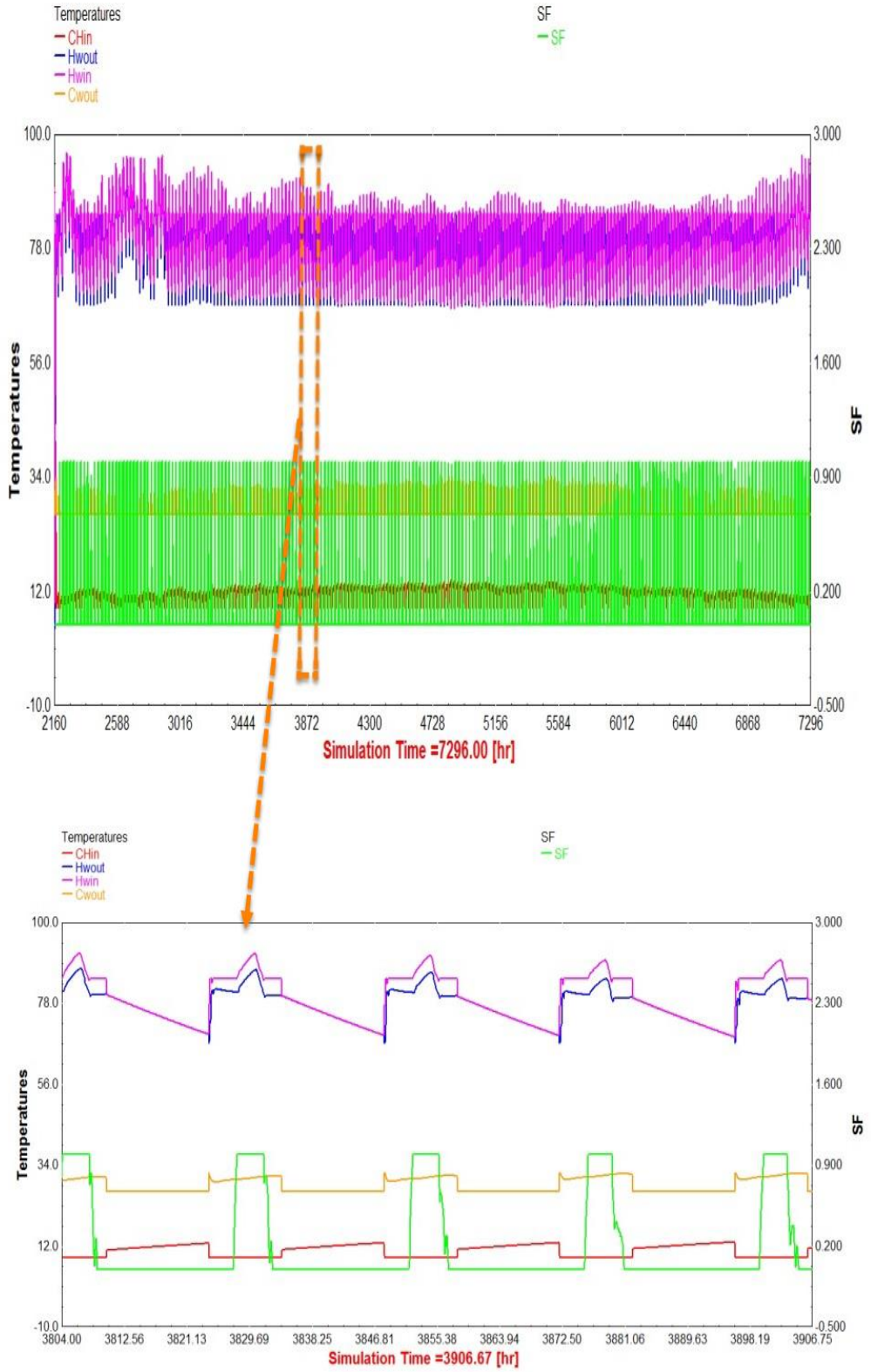

Figure 3-7 The temperatures of hot water, cooling water and chilled water in the adsorption chiller and the solar fraction

3.5 Building Description and the Cooling Load

A diagram of the ‘solar house’ is shown in Figure 3-8, and the house is located in Baghdad the capital city of Iraq. The materials used to build the house were bricks of 12 cm and 24cm for inner and outer walls, respectively. The total area of the building is 600 m², and it includes four bedrooms, and two bathrooms located to the east side, because solar radiation enters the rooms only during morning. The living room is in the south side with large windows in order to take the benefit of the different solar altitude during the year. Furthermore, the west side of the house in summer time obtains a high amount of solar radiation. Therefore, the machinery and storage rooms are arranged in the west side. The original air conditioning system used for this building was an absorption system (A. Al-Karaghouli, 1989; Joudi & Abdul-Ghafour, 2003), whereas, in the present study an adsorption chiller has been selected and investigated.

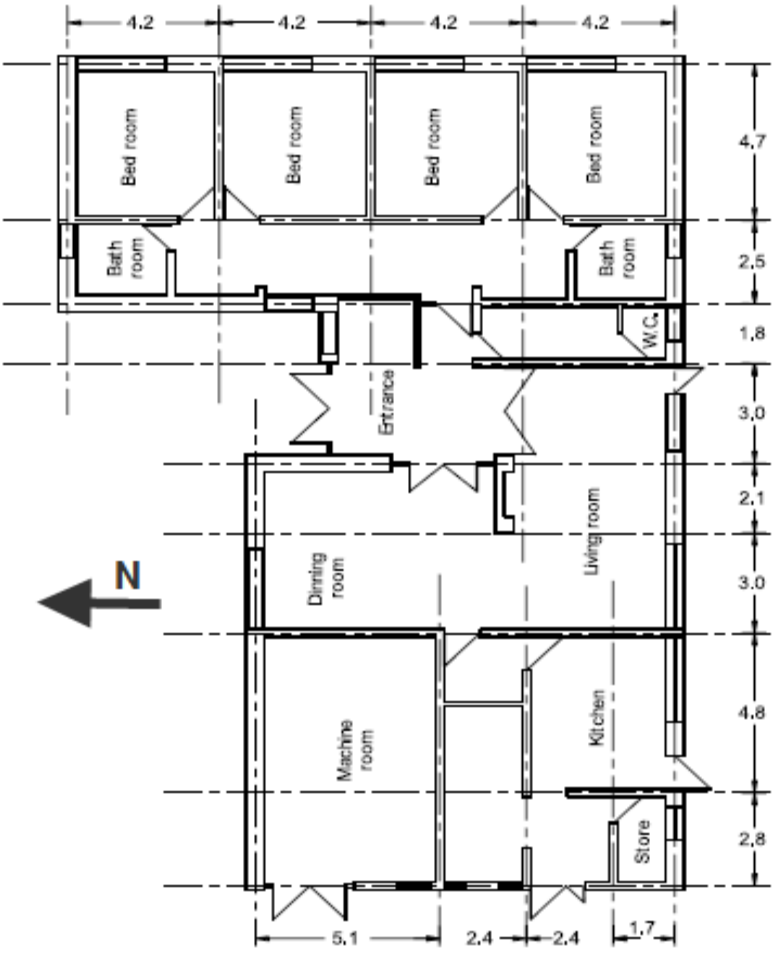

Figure 3-8 Iraqi solar house layout (Joudi & Abdul-Ghafour, 2003)

The cooling load has been simulated by using Type 682, with the data of the cooling load written in a file which Type 9e can read and convert into appropriation units, and then provide it as an input cooling load into the chilled water circuit. Figure 3-9 below shows the annual cooling load simulated.

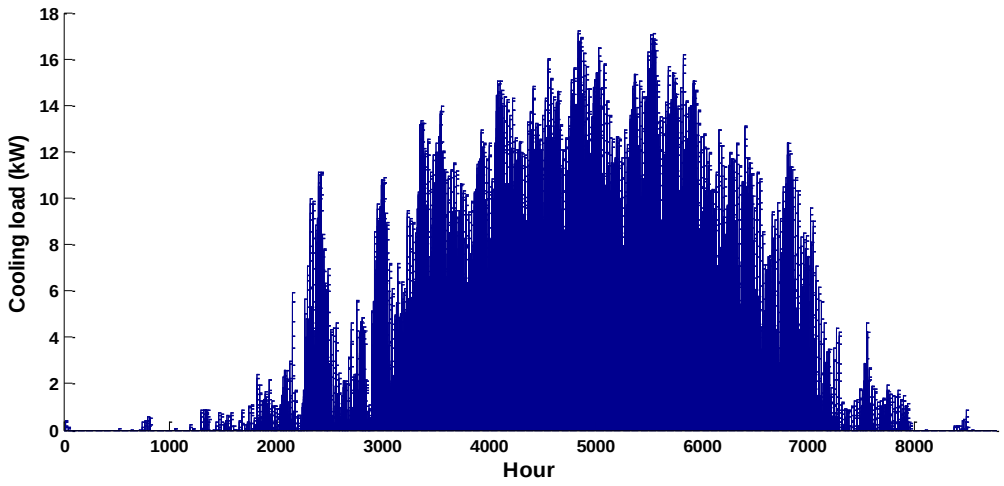

Figure 3-9 The annual cooling load profile

3.6 Climate conditions of Baghdad

Baghdad city has a subtropical arid climate, where the total annual solar radiation on a horizontal surface is higher than 7000 MJ/m^2.year (Al-Helal, 2015), with over 3000 hours of bright sunshine (Alasady, 2011). Figure 3-10 shows the position of Iraq in an area of over 3000 hours of bright sunshine.

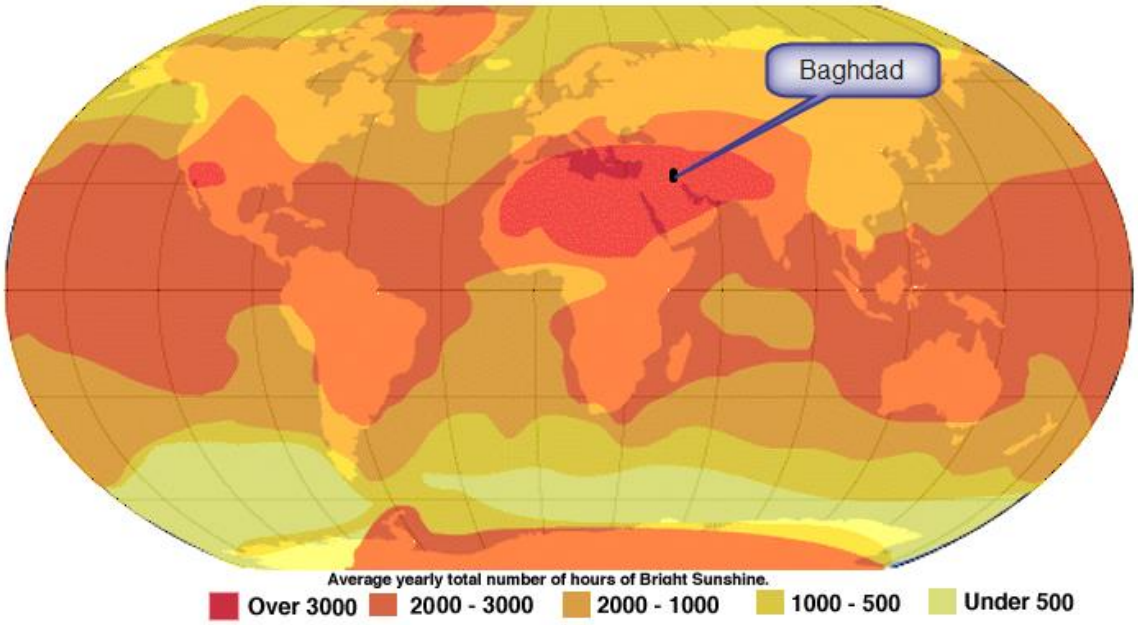

Figure 3-10 Average yearly total hours of bright sunshine (Alasady, 2011)

In summer from June to August, the average maximum temperature is as high as 44 °C, along with blazing sunshine. Baghdad could be considered as one of the hottest cities in the world; even at night temperatures are rarely below 24 °C. Baghdad's record highest temperature of 51 °C was reached in July 2015. In winter, it is characterised by mild days and chilly nights. From December to February, Baghdad has maximum temperatures averaging 15.5 to 18.5 °C, although there may be highs above 21 °C. Figure 3-11 illustrates the sunshine duration and the temperature of Baghdad city during the months of the year where the highest temperature and longest sunshine hours occur, in June, July and August. Figure 3-12 shows the monthly mean daily global solar radiation and the day length of Baghdad in hours, where the highest solar radiation was in June. All the data in the Figures is from Al-Salihi (2010).

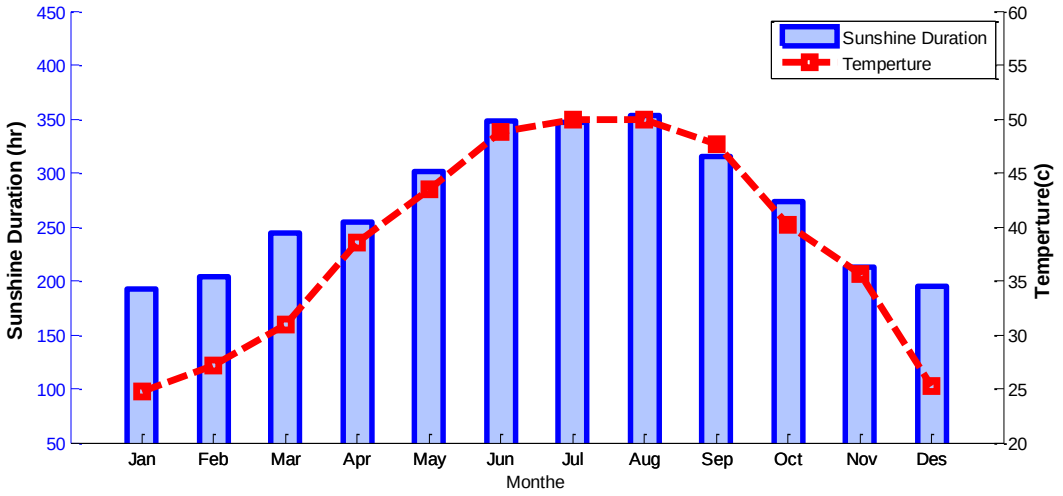

Figure 3-11 The average sunshine duration (hr) and the temperature of Baghdad city during the months of the year

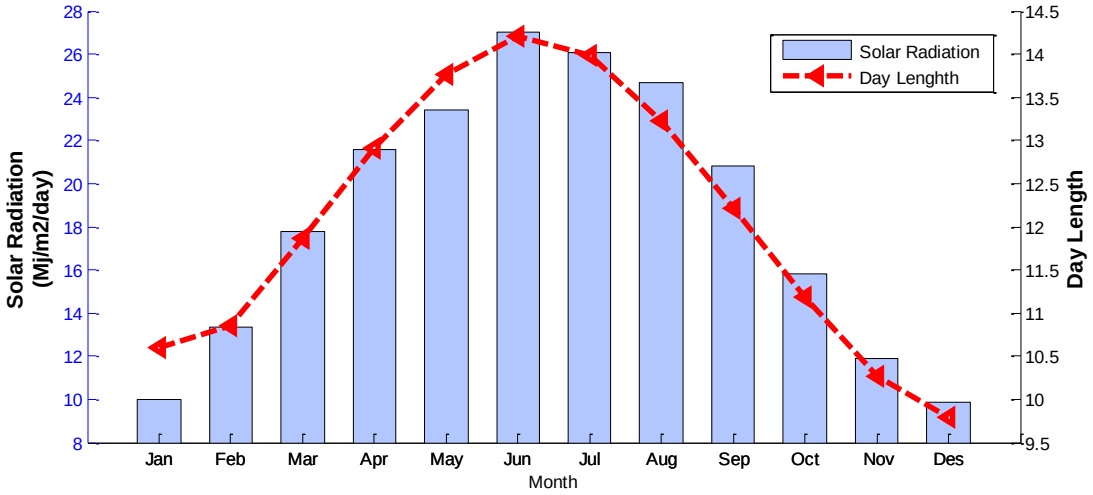

Figure 3-12 The solar radiation (MJ/m^2/day) and the day length of Baghdad city during the months of the year

3.7 Summary

In Chapter Three the solar adsorption cooling system was modelled using the TRNSYS simulation programme. In TRNSYS software the component was chosen to model the system in the simulation studio. The component types used were Type 71 for the evacuated tube solar collector, Type 4a for the thermal energy storage tank, Type 6 for the auxiliary heater, Type 909 for the adsorption chiller, and Type 51 for the cooling tower. Moreover, there are three controllers used in the modelling of the system, first to control the flow through the

collector, second to control the hot water outlet from the chiller, and third to control the time operation of whole system. After completing the modelling on TRNSES software, the first result of the simulation was shown in Figure 3-7. Furthermore, the building description, cooling load and climate condition of Baghdad city has been described in detail.

Chapter Four

System Analysis

4.1 Introduction

Thermo-economic modelling of the solar adsorption cooling system is presented in this Chapter on the basis of exergy and economic analysis. Exergy or availability is defined as the maximum available work that can be produced by a system when it interacts with its surrounding environment. The importance of the exergy analysis was presented by Hepbasli (2008) through the following points: "(a) it is a primary tool in best addressing the impact of energy resource utilization on the environment. (b) It is an effective method using the conservation of mass and conservation of energy principles together with the second law of thermodynamics for the design and analysis of energy systems. (c) It is a suitable technique for furthering the goal of more efficient energy–resource use, for it enables the locations, types, and true magnitudes of wastes and losses to be determined. (d) It is an efficient technique revealing whether or not and by how much it is possible to design more efficient energy systems by reducing the inefficiencies in existing systems. (e) It is a key component in obtaining a sustainable development". Moreover, in (2010), he indicated that in the simulation for the thermodynamic analysis of energy systems, the most powerful tool is exergy analysis.

During recent years, many studies on exergy and economic analysis have been carried out for solar cooling systems. Zhai et al. (2009) applied the Second Law of Thermodynamics in order to evaluate the exergy efficiency of a small-scale novel hybrid solar cooling and heating system under Chinese climate conditions. They found that the highest exergy destruction was in the solar collector. Onan et al. (2010) studied the hourly exergy loss of a solar assisted absorption refrigeration cooling system. It was observed that the solar collector showed the greatest exergy loss. Baiju & Muraleedharan (2012) presented the exergy efficiency and exergy destruction of a solar adsorption refrigeration system working with an activated carbon-methanol pair. Baiju & Muraleedharan (2013), using a solar hybrid adsorption refrigeration system with 50L of hot water as well as 10L cold water storage, calculated the irreversibility and exegetic efficiency for each component, and it was shown that the adsorption bed and the solar collector were the main sources of irreversibility.

Rafique et al. (2016) studied the exergy analysis of a solar desiccant cooling system and the results showed that the desiccant wheels and solar collector accounted for the higher part of the exergy destruction.

4.2 Exergy Analysis

The method of exergy analysis is based on the Second Law of Thermodynamics and it focuses on the quality of the energy. In order to analyse the exergy assessment for the adsorption cooling system, the following principal equations are used to determine the exergy destruction for each component. The total exergy of the system can be separated into physical exergy (PH), potential exergy (PT), kinetic exergy (KN) and chemical exergy (CH), which can be written as Equation 4-1 (Dincer & Kanoglu, 2010; Hepbasli, 2008).

$$\dot{E}x = \dot{E}x^{PH} + \dot{E}x^{PT} + \dot{E}x^{KN} + \dot{E}x^{CH} \qquad \text{Equation 4-1}$$

In this study potential and kinetic exergy have been ignored, and the chemical exergy is set to zero because there is no any chemical reaction in the system (Aman, Ting & Henshaw, 2014).

The exergy balance equation for each component in the system can be written as:-

$$\sum \dot{E}x_{in} = \sum \dot{E}x_{out} + \dot{E}x_{des} \qquad \text{Equation 4-2}$$

Or

$$\dot{E}x_{heat} - \dot{E}x_{work} + \dot{E}x_{mass,in} - \dot{E}x_{mass,out} = \dot{E}x_{des} \qquad \text{Equation 4-3}$$

Where:-

$$\dot{E}x_{heat} = \sum \left(1 - \frac{T_o}{T_k}\right)\dot{Q}_k$$

$$\dot{E}x_{work} = \dot{W}$$

$$\dot{E}x_{mass,in} = \sum \dot{m}_{in} * \varphi$$

$$\dot{E}x_{mass,out} = \sum \dot{m}_{in} * \varphi$$

Where:-

(T_o) is ambient temperature (K).

$\left(\dot{Q}_k\right)$ is a rate of heat transfer at boundary temperature (kJ/hr).

$\left(\dot{W}\right)$ is the work rate (kW).

(T_k) is thermodynamic average temperature (boundary temperature) (Tsatsaronis, 1993):-

$$T_k = \frac{h_{out} - h_{in}}{s_{out} - s_{in}} \qquad \text{Equation 4-4}$$

$(\dot{m}_{in}, \dot{m}_{out})$ is the inlet and outlet mass flow rate (kg/hr).

(φ) is a specific unit exergy (kJ/kg), can be expressed in Equation 4-5, (Onan, Ozkan & Erdem, 2010).

$$\varphi = (h - h_o) - T_o(s - s_o) \qquad \text{Equation 4-5}$$

Where:-

(h) is the specific enthalpy, (s) is specific entropy.

The changing of entropy and enthalpy for the stream is calculated by Equations 4-6 and 4-6 (Bejan, 2006).

$$\Delta s = \int_1^2 Cp(T)dT/T \cong Cp_{avg} \ln\frac{T_2}{T_1} \qquad \text{Equation 4-6}$$

$$\Delta h = Cp_{avg}(T_2 - T_1) \qquad \text{Equation 4-7}$$

By combining Equation 4-6 with the flow specific exergy Equation 4-5, the final expression can be written as Equation 4-8:-

$$\varphi = \left[(h - h_o) - T_o\left(Cp_{avg} \ln\frac{T}{T_o} - s_o\right)\right] \qquad \text{Equation 4-8}$$

A general form of physical exergy for incompressible fluids (liquids) is defined as follows (Sanaye & Shirazi, 2013):-

$$\dot{E}x^{PH} = \dot{m}CpT_o\left[\frac{T}{T_o} - 1 - \ln\left(\frac{T}{T_o}\right)\right]$$ Equation 4-9

By obtaining the physical exergy in Equation (4-9), for each component in the system such as solar collector, hot storage tank, auxiliary heater, adsorption chiller, cooling tower and cold storage tank at ambient temperature (dead state) 25˚C at pressure (1atm), the amount of exergy destruction (irreversibility) can be calculated. Additionally, Table 4-1 lists all the exergy destruction equations for the components of the solar adsorption cooling system. All the equations of exergy destruction and exergy efficiency can be found in Gebreslassie, Medrano & Boer (2010); Hepbasli (2007); Hepbasli (2008); and Onan, Ozkan & Erdem (2010).

Table 4-1 The exergy destruction correlation used for a solar adsorption cooling system.

component	Exergy destruction equations
Solar collector	$\dot{E}xdes,sol = \dot{m}_s(\varphi 1 - \varphi 2) + \dot{Q}_s(1 - \frac{To}{Ts})$
Hot storage tank	$\dot{E}xdes,Htank = [\dot{m}s(\varphi 2 - \varphi 1) + \dot{m}ch(\varphi 3 - \varphi 4)]$
Auxiliary heater	$\dot{E}xdes,aux = \dot{m}ch(\varphi 5 - \varphi 6) + \dot{Q}aux\ (1 - \frac{To}{Taux})$
Adsorption chiller	$\dot{E}xdes,chill = [\dot{m}ch(\varphi 6 - \varphi 7) + \dot{m}ct(\varphi 8 - \varphi 9) + \dot{m}l(\varphi 10 - \varphi 11]$
Cooling tower	$\dot{E}xdes,Ct = \dot{m}ct * (\varphi 9 - \varphi 8) + \dot{W}f,ct$
Cold storage tank	$\dot{E}x\ des,ctank = \dot{m}l(\varphi 11 - \varphi 10) + \dot{m}ll(\varphi 13 - \varphi 12)$

- **For the Solar Collector :**

The exergy destruction (irreversibility) of the solar collector can be calculated as (Onan, Ozkan & Erdem, 2010). The numbers in the figure below relate to Figure 3-1 page 19:-

$$\dot{E}x_{des,sol} = \dot{m}_{sol}(\varphi_1 - \varphi_2) + \dot{Q}_s\left(1 - \frac{T_o}{T_s}\right)$$ Equation 4-10

Where:

$\left(\dot{E}x_{des.sol}\right)$ is the exergy destruction of the solar collector (kJ/hr)

$\left(\dot{m}_{sol}\right)$ is mass flow rate in the solar loop (kg/hr).

$\left(\dot{Q}_s\right)$ is amount of heat transfer (kJ/hr).

$\left(T_s\right)$ is thermodynamic average temperature (K).

Moreover, the collector has exergy absorbed from the Sun and the useful delivered exergy of the collector can be calculated from the equations below in order to find the exergy efficiency (Hepbasli, 2008).

$$\dot{E}x_u = \dot{m}_{sol}\left[\left(h_{w,out} - h_{w,in}\right) - T_o\left(s_{w,out} - s_{w,in}\right)\right] \quad \text{Equation 4-11}$$

Or

$$\dot{E}x_u = \dot{m}_{sol}\, Cp_w\left[\left(T_{w,out} - T_{w,in}\right) - T_o\left(\ln\left(\frac{T_{w,out}}{T_{w,in}}\right)\right)\right] \quad \text{Equation 4-12}$$

And the exergy of solar radiation is determined by Equation 4-13 (Caliskan, Dincer & Hepbasli, 2012) :-

$$\dot{E}x_{sra} = AI_T\left[1 + \frac{1}{3}\left(\frac{T_o}{T_{sr}}\right)^4 - \frac{4}{3}\left(\frac{T_o}{T_{sr}}\right)\right] \quad \text{Equation 4-13}$$

Where:-

$\left(T_{w,in}, T_{w,out}\right)$ is the inlet and outlet temperature of the solar collector in (K).

$\left(A\right)$ is the area of the collector (m^2)

$\left(I_T\right)$ is global solar radiation ($kJ/hr.m^{2)}$

$\left(T_o\right)$ is ambient temperature (K)

$\left(T_{sr}\right)$ is solar radiation temperature, taken to be ≈ 6000k (Petela, 2003).

The Second Law efficiency of the solar collector can be calculated according to Equation 4-14 (Onan, Ozkan & Erdem, 2010).

$$\eta_{sol} = 1 - \frac{\dot{E}\, x_{des,sol}}{\dot{E}\, x_{sra}}$$ Equation 4-14

- **For the Hot Water Tank :**

The energy is transferred from the solar collector to the hot storage tank and then the hot water is delivered to the adsorption chiller; and the equation of exergy destruction for the tank is (Hepbasli, 2007; Onan, Ozkan & Erdem, 2010):-

$$\dot{E}\, x_{des,hot\_tank} = \left[\dot{m}_{sol}(\varphi_2 - \varphi_1) + \dot{m}_{chill}(\varphi_3 - \varphi_4) \right]$$ Equation 4-15

Where: -

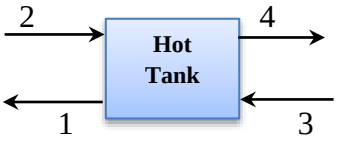

$\left(\dot{E}\, x_{des,hot\_tank} \right)$ is exergy destruction of the hot storage tank (kJ/hr).

$\left(\dot{m}_{sol} \right)$ is mass flow rate in the solar loop (hot side of the tank) (kg/hr).

$\left(\dot{m}_{chill} \right)$ is mass flow rate in the chiller loop (load side of the tank) (kg/hr).

The second law efficiency of the hot storage tank is calculated from Equation 4-16.

$$\eta_{hot\_tan} = \frac{\dot{m}_{chill}(\phi_4 - \varphi_3)}{\dot{m}_{sol}(\varphi_2 - \varphi_1)}$$ Equation 4-16

- **For the Auxiliary Heater** :

The auxiliary heater is used to boost the temperature of the hot water when it falls below the set point (85^{o}C). The exergy destruction equation for the auxiliary heater is (Hepbasli, 2007; Onan, Ozkan & Erdem, 2010):-

$$\dot{E}\, x_{des,aux} = \dot{m}_{chill}(\varphi_5 - \varphi_6) + \dot{Q}_{aux}\left(1 - \frac{T_o}{T_{aux}}\right)$$ Equation 4-17

Where: -

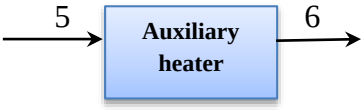

$\left(\dot{E}x_{des,aux}\right)$ is the exergy destruction of the auxiliary heater (kJ/hr).

$\left(\dot{Q}_{aux}\right)$ is heating rate of the auxiliary heater (kJ/hr).

The second law efficiency of the auxiliary heater is:-

$$\eta_{aux} = \frac{\dot{m}_{chill}\left(\varphi_6 - \varphi_5\right)}{\dot{Q}_{aux}\left(1 - \frac{T_o}{T_{aux}}\right)}$$ Equation 4-18

- **For the Chiller** :

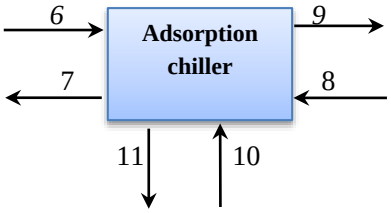

The exergy destruction of the chiller can be written as the equation below, because TRNSYS software deals with the chiller as one component (Gebreslassie, Medrano & Boer, 2010; Onan, Ozkan & Erdem, 2010).

$$\dot{E}x_{des,chill} = \left[\dot{m}_{chill}\left(\varphi_6 - \varphi_7\right) + \dot{m}_{ct}\left(\varphi_8 - \varphi_9\right) + \dot{m}_{l}\left(\varphi_{10} - \varphi_{11}\right)\right]$$ Equation 4-19

Where:-

$\left(\dot{E}x_{des,chill}\right)$ is the exergy destruction of the chiller (kJ/hr).

$\left(\dot{m}_{ct}, \dot{m}_{l}\right)$ is the mass flow rate in cooling tower loop and chilled water loop, respectively (kg/hr).

The second law efficiency of the chiller is written as:-

$$\eta_{chill} = \frac{\dot{m}_{l}\left(\varphi_{11} - \varphi_{10}\right)}{\dot{m}_{chill}\left(\varphi_6 - \varphi_7\right) + \dot{m}_{ct}\left(\varphi_8 - \varphi_9\right)}$$ Equation 4-20

- **For the Cooling Tower**:

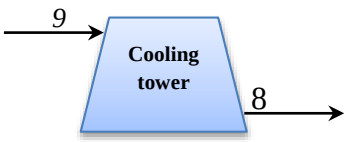

The exergy destruction of the cooling tower is the exergy rate of mass flow plus the work rate of the fan in the cooling tower (Hepbasli, 2007; Onan, Ozkan & Erdem, 2010).

$$\dot{E}x_{des,Ct} = \dot{m}_{ct}(\varphi_9 - \varphi_8) + \dot{W}_{f,ct}$$ Equation 4-21

Where:-

$\left(\dot{W}_{f.ct}\right)$ is the amount of power consumption of the fan in the cooling tower (kJ/hr).

The second law efficiency of the cooling tower is:-

$$\eta_{Ct} = \frac{\dot{m}_{ct}(\varphi_9 - \varphi_8)}{\dot{W}_{f,ct}}$$ Equation 4-22

- **For the Cold Tank**

The cold storage tank is used to store the chilled water produced from the adsorption chiller; and the exergy destruction equation is (Hepbasli, 2007; Onan, Ozkan & Erdem, 2010):-

$$\dot{E}x_{des,cold\_tank} = \dot{m}_{l}(\varphi_{11} - \varphi_{10}) + \dot{m}_{ll}(\varphi_{13} - \varphi_{12})$$ Equation 4-23

Where:

$\left(\dot{m}_{l}, \dot{m}_{ll}\right)$ is the mass flowrate of chilled water in the chiller side and load side (kg/hr), respectively.

The second law efficiency of the cold storage tank can be written as:-

$$\eta_{cold\_tan} = \frac{\dot{m}_{l}(\varphi_{12} - \varphi_{13})}{\dot{m}_{ll}(\varphi_{11} - \varphi_{10})}$$ Equation 4-24

The exergy efficiency (second law efficiency) for the complete system can be calculated as (Aminyavari et al., 2014; Navidbakhsh, Shirazi & Sanaye, 2013; Shirazi et al., 2014) :-

$$\eta_{total} = \frac{\dot{E}\, x_{out}}{\dot{E}\, x_{in}} \qquad \text{Equation 4-24}$$

Or

$$\eta_{total} = 1 - \frac{\dot{E}\, x_{des,total}}{\dot{E}\, x_{in}} \qquad \text{Equation 4-25}$$

Where:

$\left(\dot{E}\, x_{des,total}\right)$ represents the summation of the exergy destruction of the components in the system (solar collector + hot storage tank + auxiliary heater + adsorption chiller + cooling tower + cold storage tank).

$\left(\dot{E}\, x_{in}\right)$ is the exergy of solar radiation in the collector, the exergy of the auxiliary heater and the summation of the power consumption for the all pumps in the system, including the power consumption in the fan of the cooling tower.

4.3 Economic Analysis

Economic feasibility for a solar adsorption cooling system is essential to help the system to be more attractive by minimizing the operation cost, as well as the investment and maintenance costs of the system.

4.3.1 Investment cost rate

The Hourly Cost Rate of Investment and Maintenance includes the cost rate for the equipment of the solar thermal adsorption cooling system (collector, hot storage tank, auxiliary heater, chiller, cooling tower, cold storage tank, and pumps). The investment cost rate (US$/hr) can be calculated by the equation below in the ‘kth’ system component (Sanaye & Shirazi, 2013).

$$Z^{\bullet}_{k} = \frac{Z_k * crf * \phi}{N}$$ Equation 4-26

Where:-

(Z_k) is capital cost (US$).

(crf) is a capital recovery factor.

(ϕ) is a maintenance factor (assumed 1.06 (Kwak, Kim & Jeon, 2003)).

(N) is the operation hours of the system (hr).

Capital recovery factor (*crf*) can be calculated by the function below (Caliskan, Dincer & Hepbasli, 2013):-

$$crf = \frac{ir(ir+1)^n}{(ir+1)^n - 1}$$ Equation 4-27

Where:-

(ir) is interest rate, assumed to be 6% in Iraq ('Trading Economics,').

(n) is number of years or life span (assumed to be 20 years (Eicker & Pietruschka, 2009; Hang, Qu & Zhao, 2011)).

The Levelized Energy Cost method (Caliskan, Dincer & Hepbasli, 2013; Kwak, Kim & Jeon, 2003) was used to estimate the capital cost (*Z*κ in US$) for all components in the system (Caliskan, Dincer & Hepbasli, 2013).

$$Z_k = PW$$ Equation 4-28

Where:-

(PW) is amortization cost for the component (US$) and is equal to:-

$$PW = C - sv(pwf)$$ Equation 4-29

$$pwf = \frac{1}{(1+ir)^n}$$ Equation 4-29a

$$sv = C\mu$$ Equation 4-29b

Where:-

(pwf) is the present worth factor.

(sv) is salvage value (US$).

(μ) is the salvage value percentage (taken 15%) (Caliskan, Dincer & Hepbasli, 2013).

(C) is total capital cost of investment (US$) and it can be taken from the table below.

Table 4-2 The initial cost of the main equipment.

Components	Cost	Unit
Adsorption chiller (Jakobe, 2014)	2890	US$/kW
Solar collector (Al-Alili et al., 2010)	502	US$/m²
Storage tank (Tsoutsos et al., 2010)	600	US$/$m^3$
Cooling tower (Al-Alili *et al.*, 2010)	68	US$/kW
Auxiliary heater (Tsoutsos *et al.*, 2010)	50	US$/kW
Pumps (Al-Alili *et al.*, 2010; Gebreslassie et al., 2009)	$881(w)^{0.4}$	US$

4.3.2 **Operation cost rate**

The operation cost rate (US$/hr) represents the amount of power consumption on all pumps and fans multiplied by to the cost of electricity (US$/kW.hr) which is assumed to be 0.02$/kW.hr ('Ministry of Electricity of Iraq,').

$$C^{\bullet}_{op} = \left(\dot{W}_{pump1} + OP_{aux} + \dot{W}_{pump2} + \dot{W}_{pump3} + \dot{W}_{pump4} + \dot{W}_{pump5} + \dot{W}_{f,ct} \right) * C_{elec}$$ Equation 4-30

Where:-

$\left(\dot{W}_{pump1}\right)$ is the amount of power consumption in the solar loop pump (kW).

(OP_{aux}) is the required heating rate in auxiliary heater (kW).

$\left(\dot{W}_{pump2}\right)$ is the amount of power consumption in the pump of hot loop (chiller) (kW).

$\left(\dot{W}_{pump3}\right)$ is the amount power consumption in the pump of cold loop (cooling tower)(kW).

$\left(\dot{W}_{pump4}\right)$ is the amount of power consumption in the pump of chilled loop (kW).

$\left(\dot{W}_{pump5}\right)$ is the amount of power consumption in the pump of returning from load (kW)

$\left(\dot{W}_{f,ct}\right)$ is the amount of power consumption in the fan of cooling tower (kW).

(C_{elec}) is the electricity cost (US$/kW.hr).

Total cost rate function of the system is equal to the summation of the investment cost and operation cost, and it is defined by Equation 4-31:-

$$C^{\bullet}_{total} = \sum Z^{\bullet}_{K} + C^{\bullet}_{OP} \qquad \text{Equation 4-31}$$

This equation will be used as one of the objective functions in Chapter Six.

4.4 Summary

In Chapter Four, thermo-economic modelling of the solar adsorption cooling system has been presented on the basis of exergy and economic analysis. Firstly, the exergy destruction and exergy efficiency for each component in the system have been defined and calculated for exergy analysis. Secondly, the economic feasibility for the system was also presented by evaluating the investment and maintenance hourly cost rate for each component. Moreover, the Levelized Energy Cost method was used to estimate the capital cost for the whole system. Finally, the operation cost rate was also calculated in order to estimate the total cost rate of the system.

Chapter Five

Parametric Study

5.1 Introduction

Parametric analyses were conducted in order to evaluate the effects of some key design parameters on the system performance, such as the solar fraction, operation and investment cost, exergy destruction and exergy efficiency of the system. Four parameters were selected, based on published literature from many previous studies on solar cooling and heating systems. Mateus & Oliveira (2009) used TRNSYS to model a solar absorption system for different building types and locations. They presented the influence of ratio of hot storage tank volume to collector area on the operation cost and the solar fraction of the system. The study concluded that, only in the case of small values of the ratio of storage tank volume to collector area, the solar fraction can be increased and the operation cost reduced, while there was no significant difference in solar fraction and operation cost for large ratios. Abu Hamdeh et al. (2010) designed and developed a prototype solar adsorption refrigeration unit under Jordanian climate conditions, and studied the effects of collector area and hot storage tank volume on the performance of the system. Behbahani et al.(2013) studied the influence of hot storage tank volume and collector area on solar fraction of an adsorption system under Iranian climate conditions. The results showed that collector area has a more powerful influence on solar fraction than the storage tank size. Alam et al. (2013) showed that an adsorption chiller of 10 kW needs at least 38 m^2 of compound parabolic collector to power it up under Tokyo climate conditions. However, the system would only be able to convert less than 30% of the useful solar energy to produce a cooling effect. Moreover, a TRNSYS simulation of a solar adsorption cooling system powered by evacuated tube solar collectors for a non-residential building has been investigated by Januševičius, Streckienė & Misevičiūtė (2015). The effects of changing the area and slope of the collector on the performance and solar fraction were presented, and the study proposed a regression for the performance of the system as a function of the area and slope of the collector.

Some of the research that deals with other types of solar cooling systems has been illustrated here, due to the fact that there was no previous study made on the parametric analysis of a solar adsorption cooling system with a cold water storage tank. Hang & Qu (2010) presented

a model of a solar absorption cooling system for an office building, then studied the effect of changing the volume of hot and cold storage tanks on solar fraction of the system. The results showed that solar fraction is more sensitive to the hot storage tank than the cold storage tank. Gerstler & Tang (2011) discovered that by adding a cold storage tank the energy required for the operation of an absorption chiller was reduced.

The four design parameters selected for a parametric analysis in this study and their ranges are listed in Table 5-1.

Table 5-1 Key design parameters and their ranges.

Key Parameters	Ranges
Area collector (A_r)	50 -110 m^2
Collector slope (β)	30 - 80 ^{o}
Hot tank volume (V_h)	1 - 15 m^3
Cold tank volume (V_c)	1 - 15 m^3

5.2 Parametric Study Results

The system performance was evaluated through analyses of simulation results as part of the model based design in this study. The simulation was carried out from April to October (of TMY2 weather data file), and the simulation time step was chosen as 1 min, over a duration of 10 hours per day. Parameter analysis was performed to study the effects of variations in these key parameters, on solar fraction, operation and investment cost rate, exergy destruction and the exergy efficiency, applying the same simulation time frame over the system.

5.2.1 The effect of changing hot storage tank volume with different collector areas: -

The size of the hot storage tank determines the amount of energy can that be stored in the tank, and consequently the duration over which energy can be independently provided out of sunshine hours. During the simulation the inclination angle of the collector has been set at 33^o facing due south, the volume of the cold water storage tank has been assumed to be 1.5 m^3.

The effects on solar fraction due to a change in hot storage tank volume for different collector areas are shown in Figure 5-1. It shows that, as expected, solar fraction increases with an increase in collector area, while it generally decreases with an increase in hot storage tank

volume for each given area. The largest area solar panels should be used in order to increase the solar fraction. As can be seen from the figure, there was no significant advantage of hot storage greater than 4 m^3.

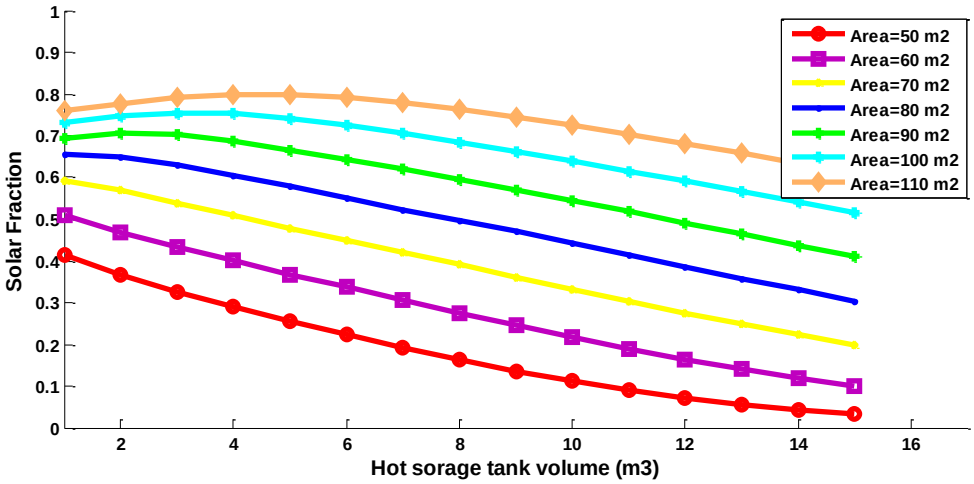

Figure 5-1 The influence of changing hot storage tank volume (m^3) on solar fraction with different collector areas (m^2)

In Figure 5-2, the effects of changing hot storage tank with different collector areas on the operation cost rate are shown. The effects on the cost are significant for large collector areas greater than 80 m^2, where the cost rate decreases as the hot storage tank volume increases. However, for areas less than 80 m^2, the operation cost decreases and then increases with increases in hot water storage volume. This demonstrates an inability of the collectors to energise large hot storage tanks sufficiently, thus as it increases in size the cost rate is increased.

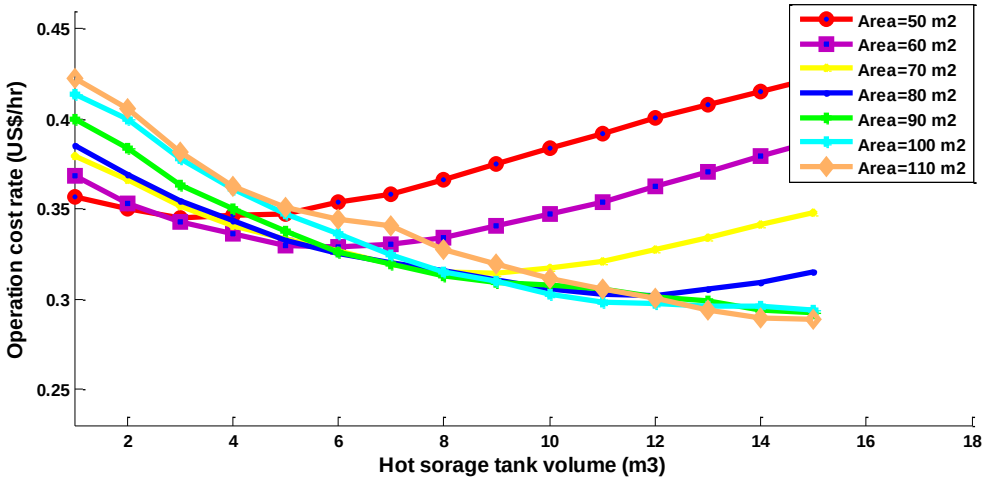

Figure 5-2 The influence of changing hot storage tank volume (m^3) on the operation cost rate (US$/hr) with different collector areas (m^2)

Figure 5-3 is presented to clarify the effects of variations in hot storage tank volume on the investment and maintenance cost rate with different collector areas. It shows that, investment and maintenance cost rate increases with an increase in the collector area and an increase in the volume of the tank, whereas, for areas greater than 90 m^2, it decreases when hot storage tank volume is less than $5m^3$. According to Equation 4-26, the variation of the investment cost rate results directly from variation of the operation hours of each component. It can be concluded from Figures 5-2 & 5-3 that the operation cost rate is much more sensitive than the investment cost rate when changing the volume of hot storage tank. Figure 5-4 shows the effects of hot storage tank volume at different collector areas on the operation cost plus investment and maintenance cost rate combined.

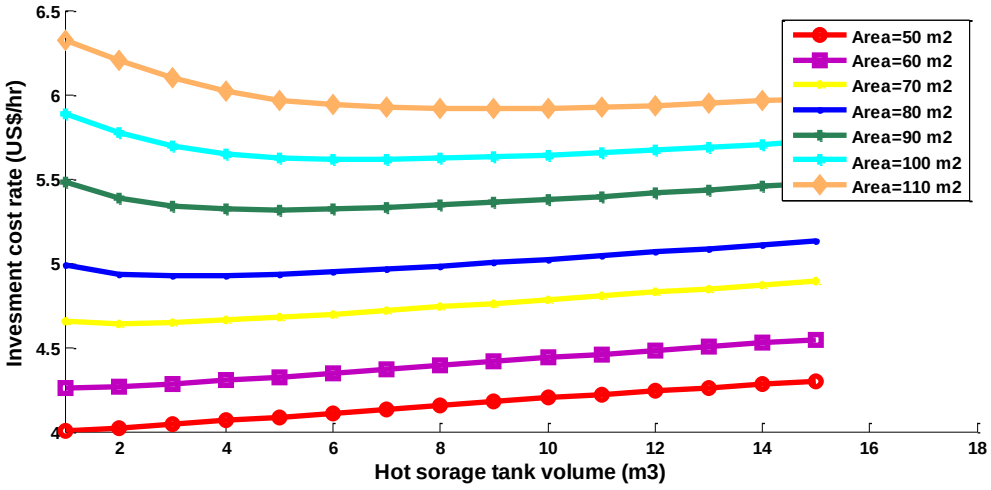

Figure 5-3 The influence of changing hot storage tank volume (m^3) on the investment cost rate (US$/hr) with different collector areas (m^2)

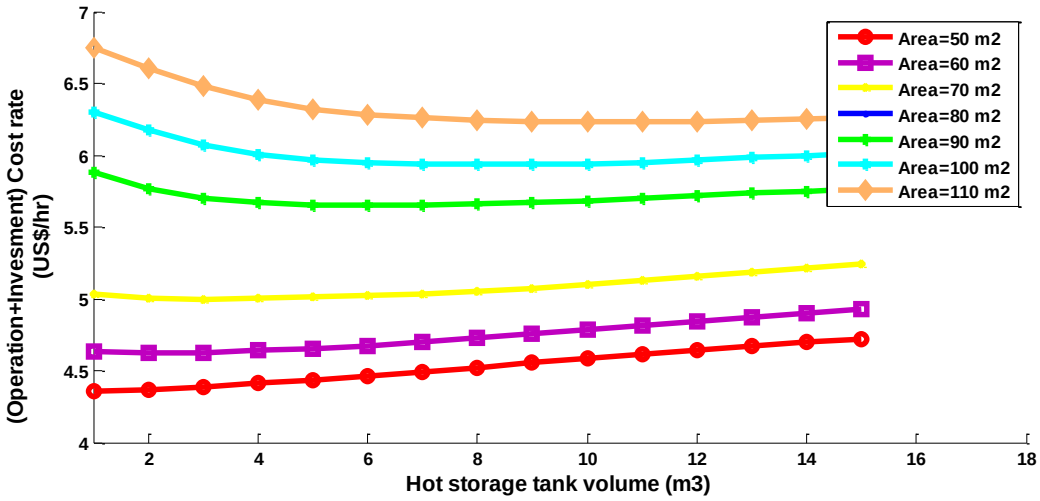

Figure 5-4 The influence of hot storage tank volume (m^3) on operation cost rate plus the investment cost rate (US$/hr) with different collector areas (m^2)

The impact of changing hot storage tank volume and collector area on system exergy destruction is presented in Figure 5-5. As shown, increasing the hot storage tank volume leads to a steady, but small, increase of exergy destruction for each collector area. Nevertheless, the exergy destruction is significantly increased by an increase in collector area. That means small collector areas are to be recommended in order to obtain low exergy destruction.

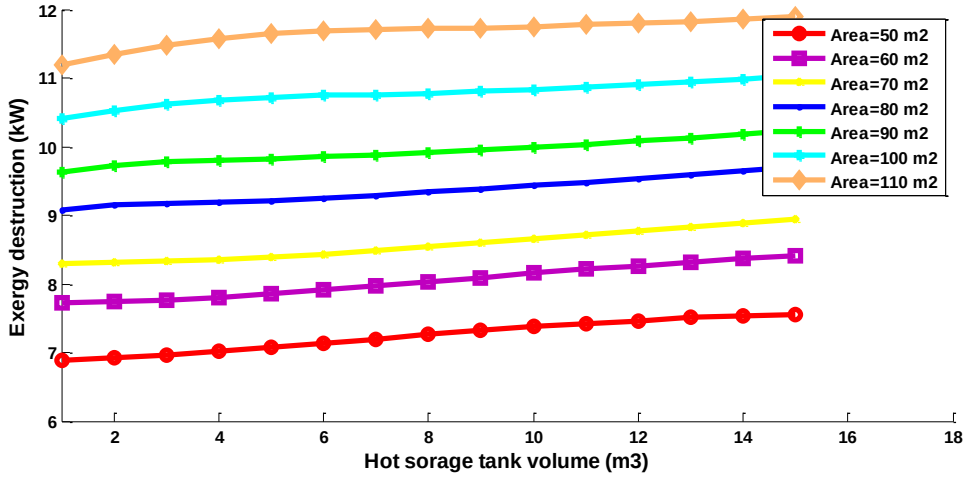

Figure 5-5 The influence of hot storage tank volume (m^3) on exergy destruction (kW) with different collector areas (m^2)

Figure 5-6 presents the results of changing hot storage tank volume on the system exergy efficiency at different collector areas. It is observed that exergy efficiency increases with an increase in collector areas. There is an optimum value of hot storage tank volume directly related to each collector area, however, the effect on exergy efficiency reaches a plateau if the volume continues to increase, and is only more effective in large areas (larger than 80 m^2).

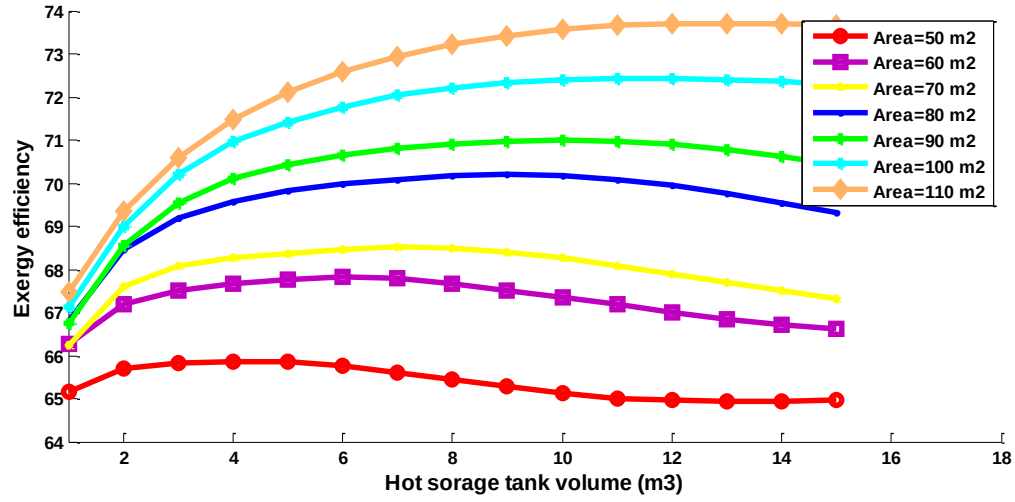

Figure 5-6 The influence of hot storage tank volume (m^3) on exergy efficiency with different collector areas (m^2)

5.2.2 The effect of changing cold storage tank volume with different collector areas: -

The size of cold storage tank represents the amount of stored chilled water that can be used when the cooling load in the building is increased. Figures presented in this section show the result of changing cold storage tank volume with different collector areas on the performance of the system. The slope of the collector and the volume of the hot storage tank have been assumed to be 33 ^{o} (due south) and 2.5m^3, respectively.

As shown in Figure 5-7, there is no influence for changing cold tank volume on solar fraction, while the solar fraction increases with an increase in the collector area. That means, as found in the literature, that solar fraction is more sensitive to the hot storage tank volume than cold storage tank volume.

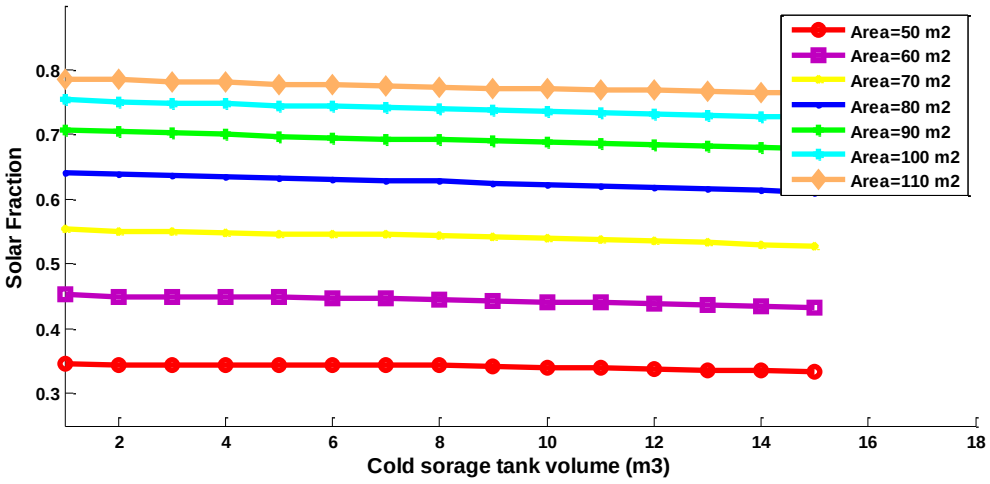

Figure 5-7 The influence of cold storage tank volume (m^3) on solar fraction with different collector areas (m^2)

Figure 5-8 confirms the impact of changing cold storage tank volume on the operation cost rate. It shows that the operation cost rate increases steadily when the volume of the cold tank is increased, more sensitively than its effect due to an increase in the area of the collector. As can be seen from the figure, there was no advantage of cold storage greater than 1 m^3.

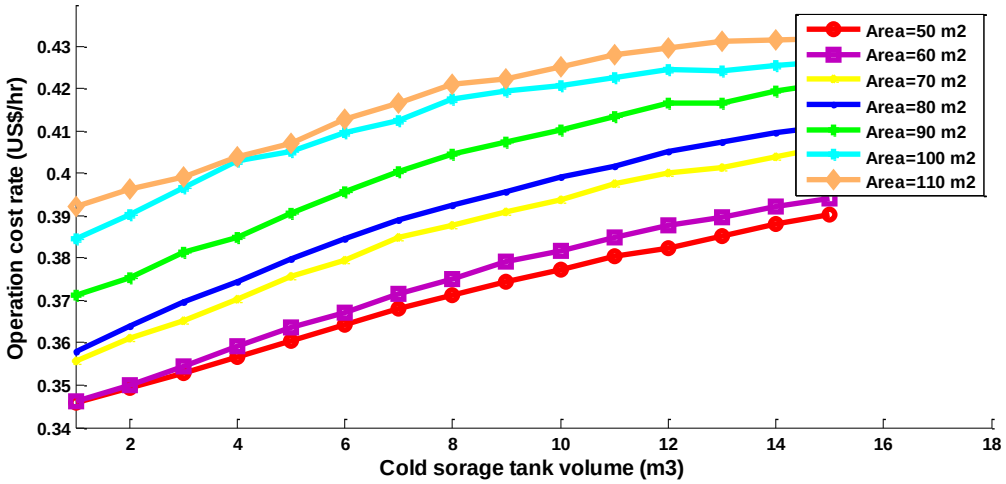

Figure 5-8 The influence of cold storage tank volume (m^3) on operation cost rate (US$/hr) with different collector areas (m^2)

Figure 5-9 shows that the investment cost rate increases with an increase in the volume of cold tank, as well as the area of the collector. Figure 5-10 presents the effect of changing the cold storage tank volume with different areas on the total (summation of operation and investment) cost rate, where it shows that the volume of the cold tank has a negative effect on the total cost rate.

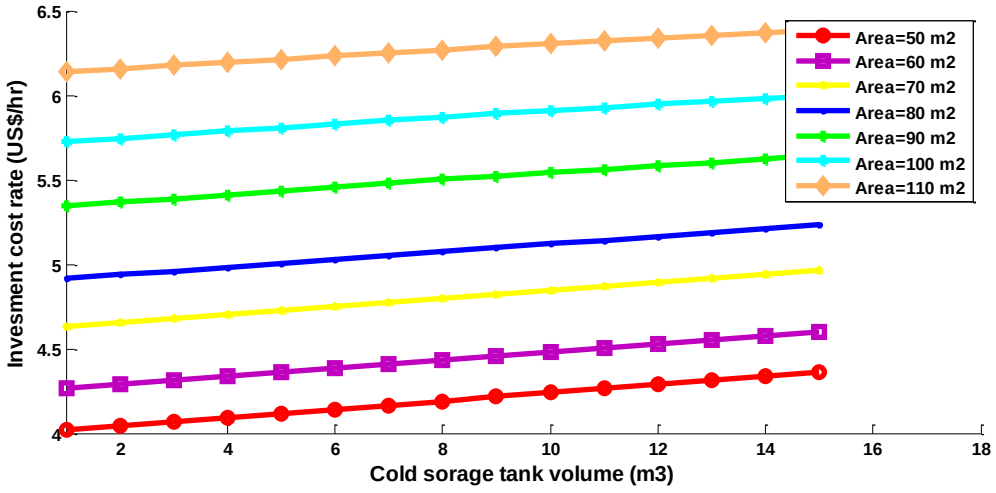

Figure 5-9 The influence of Cold storage tank volume (m^3) on the investment cost rate (US$/hr) with different collector areas (m^2)

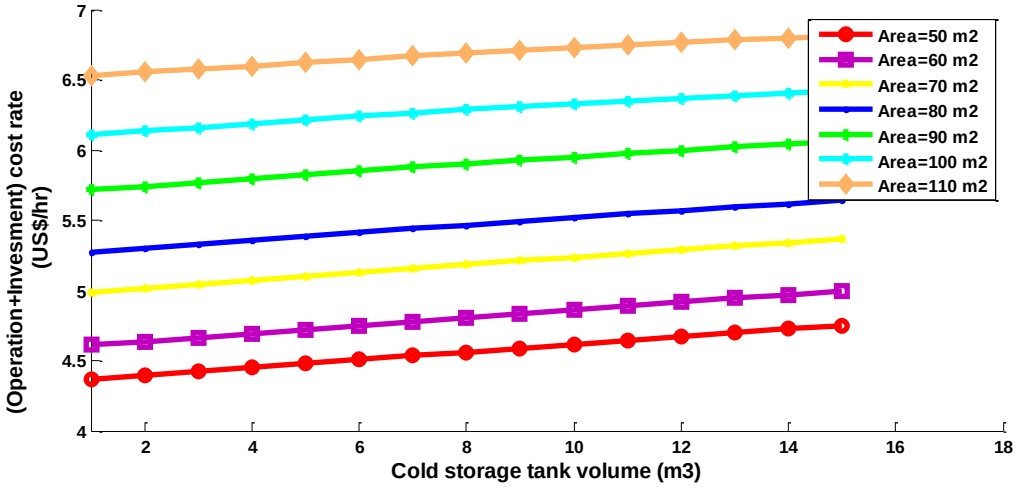

Figure 5-10 The influence of cold storage tank volume (m^3) on the operation cost rate plus the investment cost rate (US$/hr) with different collector areas (m^2)

Figure 5-11 presents the result of varying the volume of cold storage tank and the collector area on the exergy destruction of the system. It shows that there is no significant impact due to variation in cold tank volume for each area of collector, while the exergy destruction generally increases with an increase in the collector area.

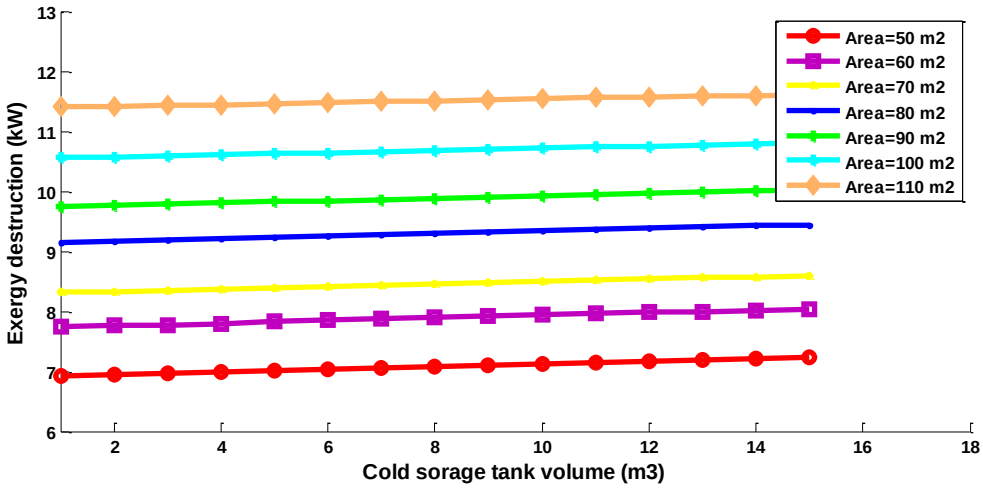

Figure 5-11 The influence of cold storage tank volume (m^3) on the exergy destruction (kW) with different collector areas (m^2)

Figure 5-12 shows that increasing the cold storage tank volume slightly reduces the exergy efficiency of the system, but the rate of decline is larger in collector areas that are less than 70m^2.

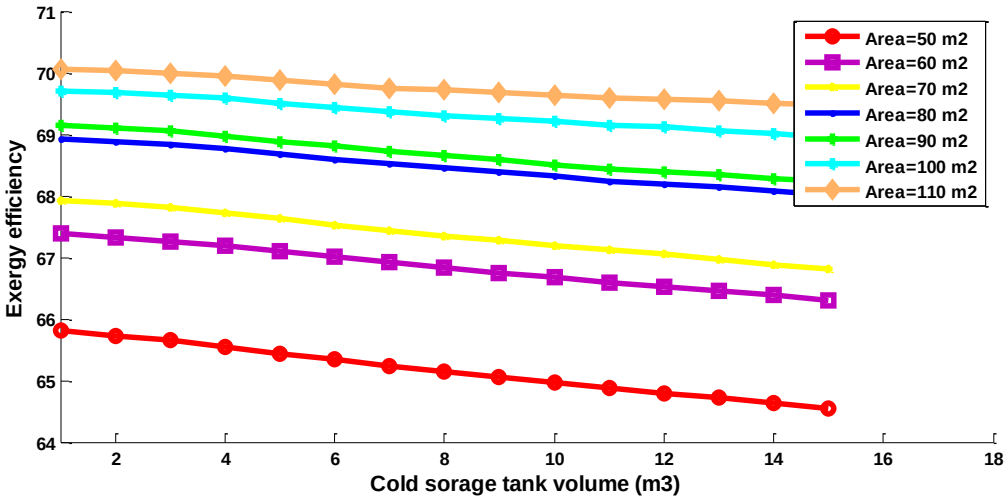

Figure 5-12 The influence of cold storage tank volume (m^3) on the exergy efficiency with different collector areas (m^2)

5.2.3 The effect of changing collector area and the collector inclination angle

The optimal inclination angle helps solar collectors to receive the greatest available amount of solar radiation. The figures in this section show how the effect of changing inclination angle and area of the collector affects the performance of the system. The volume of the hot and cold storage tank has been assumed to be 2.5m^3 and 1.5m^3, respectively.

Figure 5-13 presents the effect of changing the inclination angle with areas of the collector on solar fraction. It is obvious that solar fraction increases when the collector area increases. For areas above 70m^2 the highest solar fraction was at 30 ° and then started to slightly decrease.

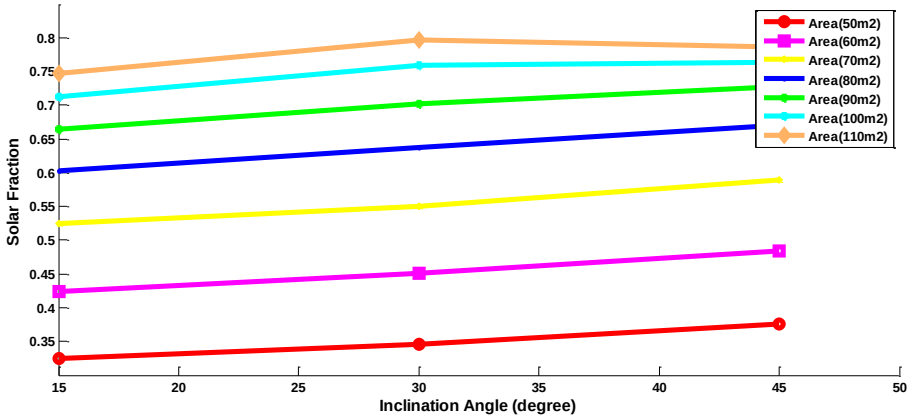

Figure 5-13 The influence of inclination angle (º) on solar fraction with different collector areas (m^2)

In Figure 5-14, the effect of changing the inclination angle of the collector with different collector areas on the operation cost rate is presented. For areas equal to and less than 60 m², there is insignificant change in the operation cost rate as the inclination angle is increased. For areas greater than 60m², there is a small increase in the operation cost rate as the slope angle is increased above 30º.

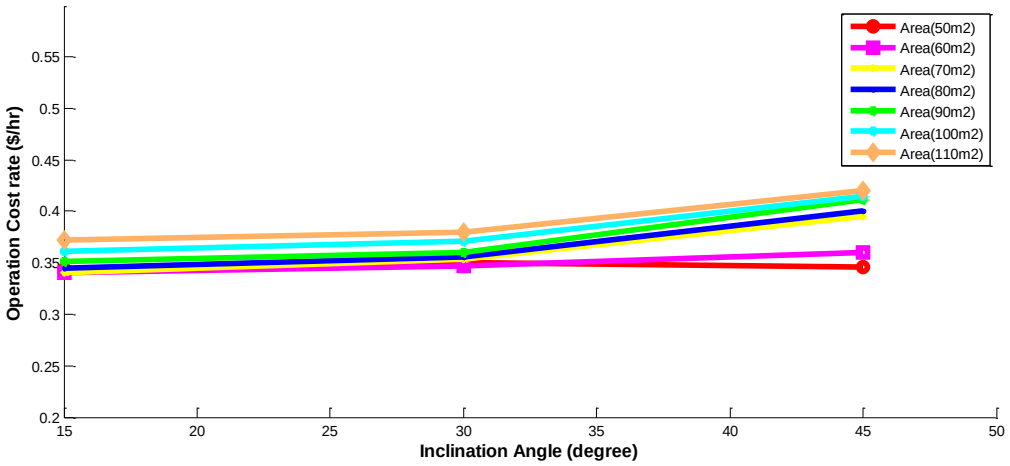

Figure 5-14 The influence of inclination angle (º) on operation cost rate (US$/hr) with different collector areas (m2)

Figure 5-15 shows that the investment cost rate is increased by increasing the collector area, whereas varying the collector inclination angle only slightly increases the investment cost rate of the system. Figure 5-16 displays the impact of inclination angle on the combined operation plus investment cost rate with different collector areas.

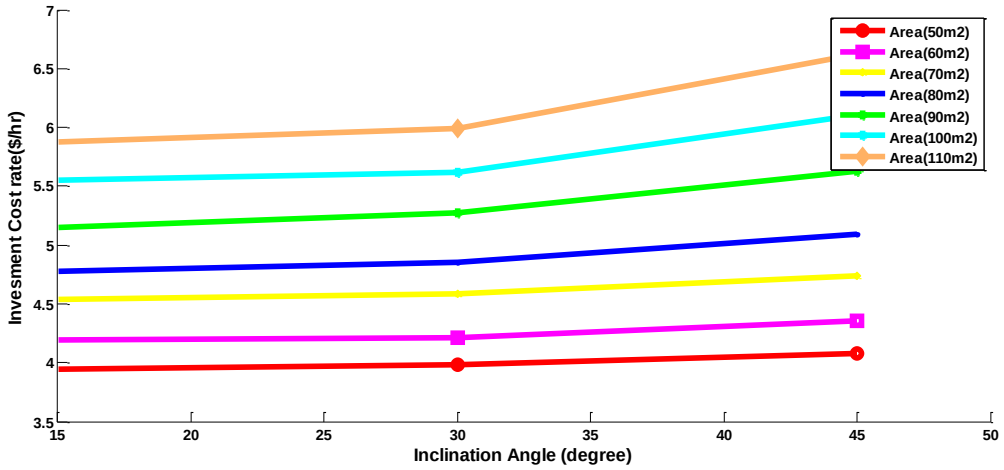

Figure 5-15 The influence of inclination angle (º) on investment cost rate (US$/hr) with different collector areas (m²)

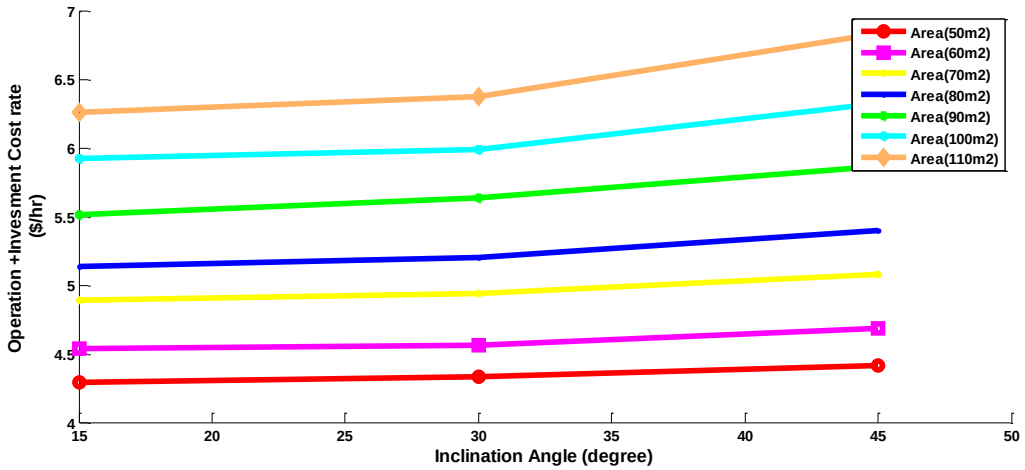

Figure 5-16 The influence of collector slope (º) on the operation plus investment cost rate (US$/hr) with different collector areas (m²)

The exergy destruction has been evaluated and presented in Figure 5-17. It shows that the exergy destruction increases with an increase in the collector area. For areas greater than 70m², there is a slight increase in the exergy destruction as the slope angle is increased above 30º.

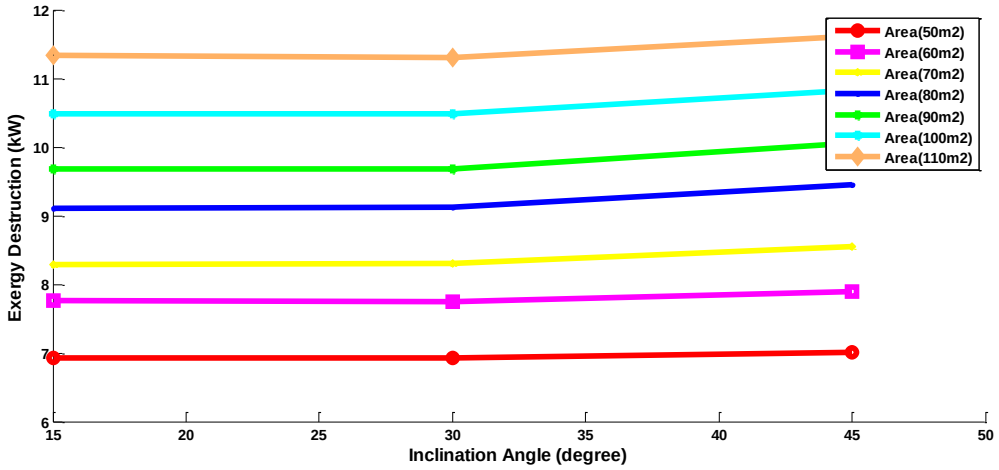

Figure 5-17 The influence of inclination angle (º) on the exergy destruction (kW) with different collector areas (m^2)

Figure 5-18 shows that the exergy efficiency increases with an increase in the collector area, whereas the exergy efficiency drops at 45º for all collector areas. As can be seen from the figure, there was no advantage of inclination angle greater than 30º.

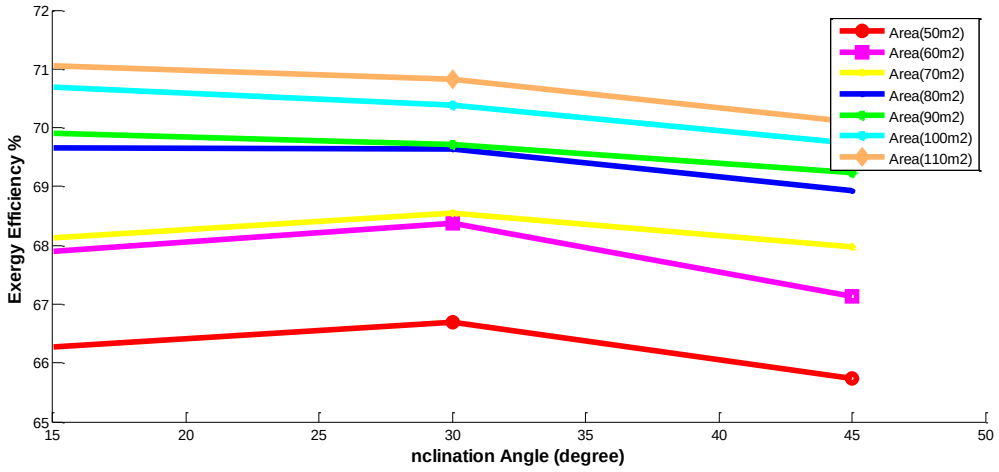

Figure 5-18 The influence of inclination angle (º) on the exergy efficiency with different collector areas (m^2)

5.3 Summary

In Chapter Five, the parametric analysis was conducted in order to assess the effect of the key parameters on the different aspects of performance (solar fraction, operation and investment cost rate, exergy destruction and exergy efficiency of the system). The effect of changing the

hot storage tank, cold storage tank and the inclination angle with different collector areas were investigated, and can be summed up as follows: -

- Solar fraction increases with an increase in collector area, while it generally decreases with an increase in hot storage tank volume for each given area.

- The operation cost rate is more sensitive than the investment cost rate when changing the volume of hot storage tank.

- Small collector areas should be recommended if low exergy destruction was to be desired.

- For large area collectors, increasing the storage volume can be a more effective improvement on system exergy efficiency.

- Solar fraction is more sensitive to hot storage tank volume than cold storage tank volume; there is no advantage of cold storage greater than $1m^3$.

- The optimal inclination angle of solar collectors is directly related to the collector area, which is essential to decrease the operation cost rate.

-There is no advantage of inclination angle greater than 30^o on investment cost rate, exergy destruction and exergy efficiency.

Chapter Six

System Optimization

6.1 Introduction

Several researchers had used parametric analyses, studying the effect of altering a single parameter on the performance of the system while the other parameters were fixed, in order to find an optimum of the system (Al-Alili *et al.*, 2010). However, the downside of this attitude is that the optimum parameter cannot be certified since the obtained results could change if any of those fixed variables changed. Moreover, it is important to optimize the complete solar adsorption system since finding the optimum adsorption cycle does not mean it would tip to find the optimal solar adsorption system. One of the main obstacles for marketing the adsorption chiller is the low performance and the size of the chiller (Alam, Saha & Akisawa, 2013), thus optimal design and operation of the whole system is very important.

Optimization process aims to find the 'best' feasible design for the system when a goal (objective), such as cost or efficiency, can be maximized or minimized under the available resources (constraints). However, most practical or real problems deal with multiple conflicting goals, which means the system must be optimized simultaneously by minimizing or maximizing more than one objective. Instead of having a single unique solution, numerous possible solutions can be produced from multi-objective optimization. These solutions are called Pareto fronts (frontiers); based on the designer's judgment, a single solution will be selected.

Hang et al.(2013) performed a multi-objective optimization for a solar cooling system by examining three design parameters (collector area, slope and hot storage tank). The advantage of using a cold storage tank was demonstrated for many other systems, when exergy and operation and capital costs were used as the objective functions (Navidbakhsh, Shirazi & Sanaye, 2013; Sanaye & Shirazi, 2013).

6.2 Coupling TRNSYS with MATLAB software

MATLAB is selected as an optimizer, using the Optimization Toolbox, which can be used to solve constrained and/or unconstrained, and single-objective or multi-objective problems. There is no multi-objective optimization tool in TRNSYS, MATLAB will need to be connected to TRNSYS software to find the optimum solutions. MATLAB can open, change and save the input files of TRNSYS, then call TRNSYS to execute simulations of the system and assist the results of TRNSYS outputs. The figure below shows the proposed optimisation simulation procedure, coupling MATLAB with TRNSYS.

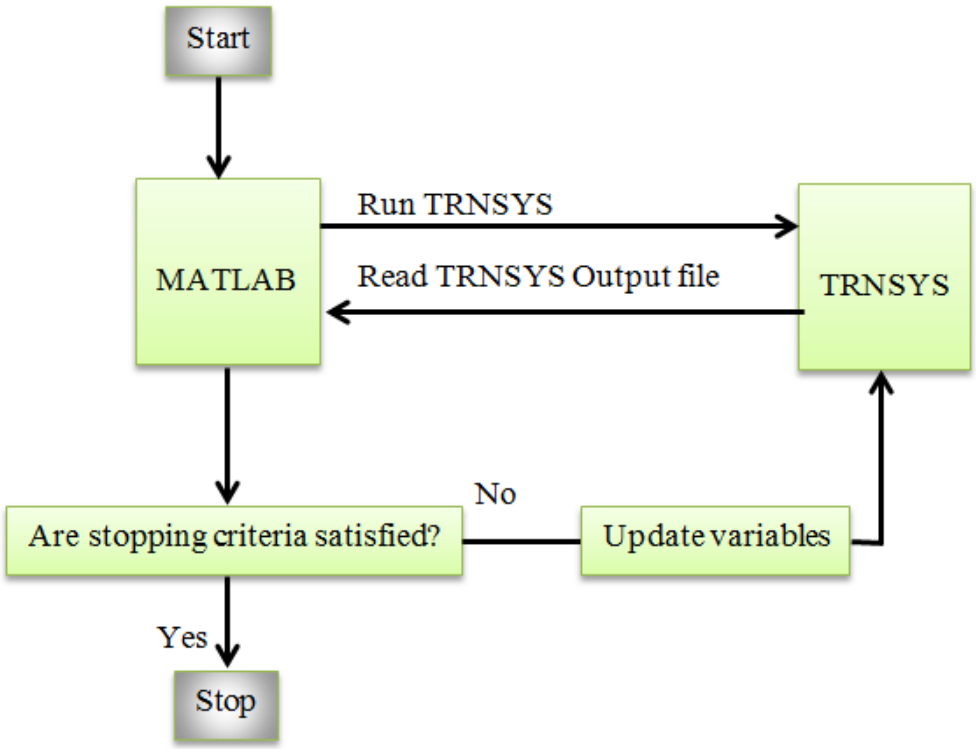

Figure 6-1 Coupling of TRNSYS with MATLAB

6.3 Genetic algorithm optimization

System optimization can be classified into two approaches: - classical methods and evolutionary methods. Evolutionary methods have unbeatable advantages in resolving complex multi-objective optimization problems. Mathematically, a multi-objective optimization problem can be defined as the minimization or maximization of the vector function below, which has (m) objectives and (n) variables (Baghernejad & Yaghoubi, 2012).

$$F(x) = F(f_1(x), f_2(x), \ldots\ldots f_m(x))$$

Where *F(x)* is the function of the variable space, such as *x* = x(x_1,…,x_n), to the points of the objective function space.

Minimize or maximize $(f_1(x), f(x)_2, \ldots\ldots f_m(x))$

Subject to $g_j(x) \geq 0 \qquad j = 1,2,\ldots\ldots, j$

$$h_k(x) = 0 \qquad k = 1,2,\ldots\ldots, k$$

$$x_i(lower) \leq x_i \leq x_i(upper) \qquad i = 1,2,\ldots\ldots, n$$

There are many optimization algorithms available to solve a multi-objective optimization problem, and one of these methods is Genetic Algorithm (GA). Genetic Algorithm is based on an analogy with Darwin's laws and it is one of the methods which solve multi-objective functions (Shirazi *et al.*, 2014).

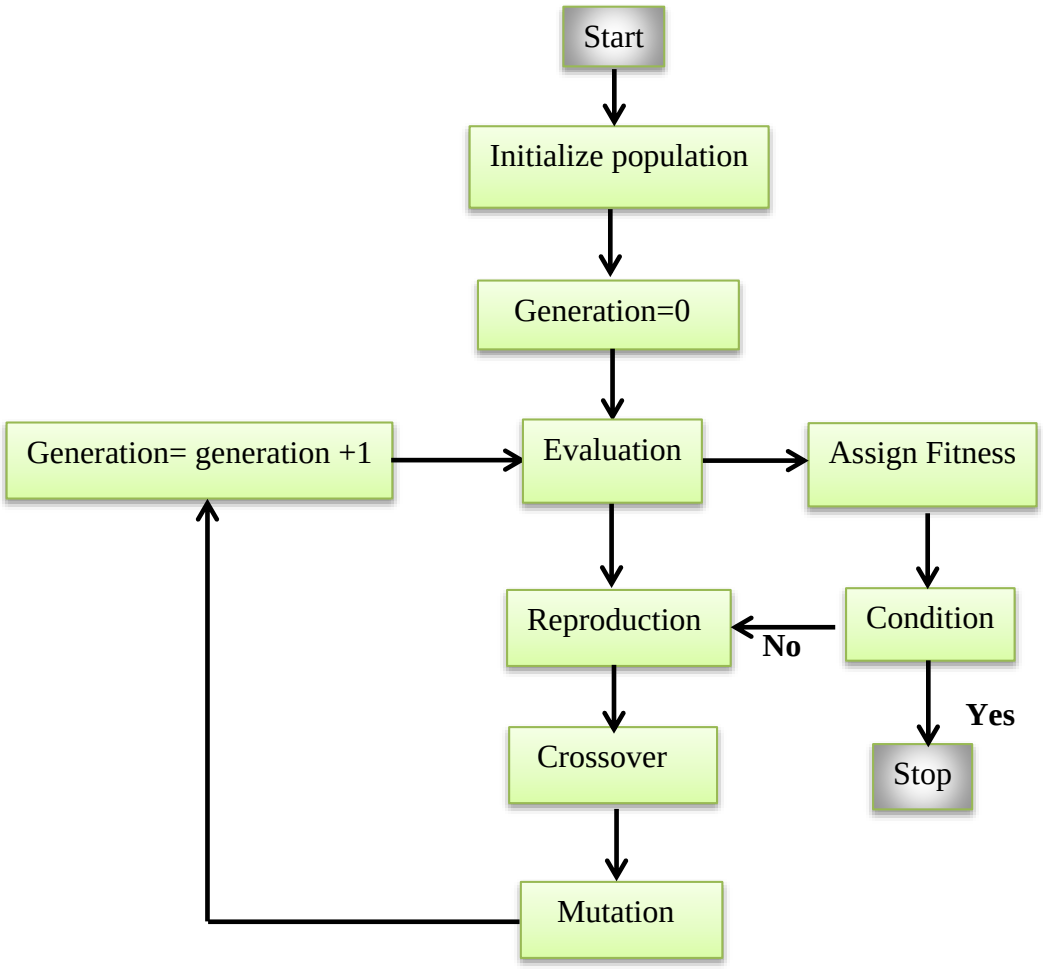

Figure 6-2 A flow chart of working principle for the genetic algorithm

The basic idea of the genetic algorithm is generating a new set of population (design variables) from a current set in order to improve the fitness (objectives). “It combines selection, crossover, and mutation operators with the goal of finding the best solution to a problem. Potential solutions are repeatedly graded on fitness and combined to produce new and potentially better solutions” (Abbaspour & Saraei, 2015). Figure 6-2 represents various stages of the genetic algorithm optimization process. Eventually, the population converges and a Pareto front optimal set is produced. Then a decision can be made to choose which of these solutions is the most suitable, or a ‘compromise’ must be made.

6.4 Objective Functions

In the present study, GA is used to optimize the two objective functions presented in Equation 4-25 (to maximize the exergy efficiency) and Equation 4-31 (to minimize the total cost rate). The Genetic Algorithm Toolbox of MATAB was used with assumptions of 400 generations with population size of 50 individuals, crossover probability 0.8 and mutation probability 0.2 (default values of multi-objective GA tool in MATLAB)

6.5 Design Variables of the Optimization

The key variables selected for optimization of the system are: - collector area (A_r), collector slope (β), hot storage tank volume (V_h) and cold storage tank volume (V_c). The ranges of variations for the individual parameters are summarized in Table 6-1.

Table 6-1 Optimization variables.

parameters	Min.value	Max.value	constraints
Area collector (A_r)	50 m²	110m²	$A_{r,min} \leq A_r \leq A_{r,max}$
Colector Slope (β)	30 °	80 °	$\beta_{,min} \leq \beta \leq \beta_{,max}$
Hot tant volume (V_h)	1 m³	15 m³	$V_{h,min} \leq V_h \leq V_{h,max}$
Cold tank volume (V_c)	1 m³	15 m³	$V_{c,min} \leq V_c \leq V_{c,max}$

6.6 Optimization results

Figure 6-3 shows the Pareto optimal solutions obtained from the multi-objective optimization of the solar adsorption system. As can be observed in this figure, the exergy efficiency of the

'optimal' system ranges from 66.0435% to 75.0417% , a difference of 14%, while the total cost rate varies from 4.3021 US$/hr to 6.3613US$/hr and this represents an difference of 48%. The final results achieved by GA optimization are illustrated in Table 6-2.

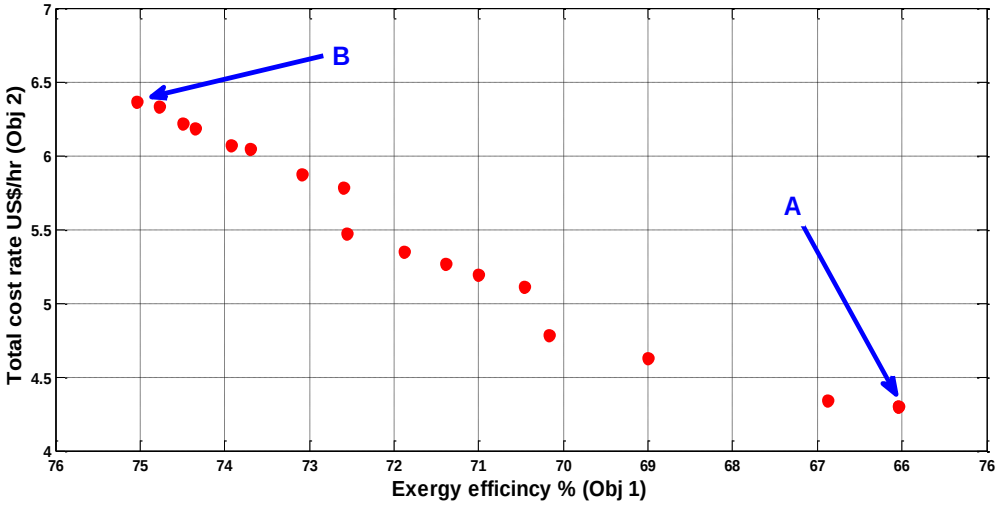

Figure 6-3 Pareto optimal frontier from multi-objective optimization of the solar adsorption cooling system

All points from the Pareto frontier can be chosen as the optimal design point of the system. As shown in Figure 6-3, if maximization of the exergy efficiency is the only goal concerned, the solution could be point B (optimum point) 75.04%. But this point will lead to the highest total cost rate 6.3613US$/hr. On the other hand, if the total cost is taken as the only desired aim, point A could be chosen as the optimum point, which has a total cost rate in the order of 4.3021US$/hr. But this point will lead to the lowest exergy efficiency 66.0435%. Therefore, a process of decision-making is required in order to find the optimum solution (Shirazi et al., 2012).

Table 6-2 The result of Genetic Algorithm optimization.

No.	Collector area(A_r) m^2	Hot tank volume(V_h) m^3	Collector slope (β) degree	Cold tank volume(V_c) m^3	Exergy efficiency %	Total cost rate (US$/hr)
A1	50	1.0	30	1.5	66.04	4.30
A2	110	9.4	56	1.2	75.04	6.36
A3	95	7.9	56	1.3	73.09	5.88
A4	90	9.2	30	1.0	72.56	5.47
A5	50	3.5	30	1.3	66.87	4.34
A6	106	8.6	55	1.3	74.50	6.22
A7	104	8.3	55	1.2	74.35	6.19

A8	76	7.0	30	1.4	70.46	5.11
A9	108	9.4	30	1.2	73.92	6.07
A10	91	8.9	54	1.3	72.60	5.78
A11	67	6.4	30	1.2	70.16	4.78
A12	79	8.0	30	1.2	71.00	5.20
A13	86	8.0	30	1.4	71.88	5.35
A14	100	8.3	52	1.4	73.69	6.05
A15	82	8.6	30	1.0	71.39	5.26
A16	109	8.5	56	1.4	74.78	6.34
A17	61	51	30	1.2	69.00	4.63

6.7 Decision-making process

As mentioned before, a multi-criteria optimisation problem requires a process of decision-making to obtain the final 'optimal' solution. There are several methods that can be used to find the optimum solution from Pareto frontier. Technique for Order Performance by Similarity to Ideal Solution (TOPSIS) is one of these decision-making methods (Ahmadi et al., 2013; Sayyaadi & Mehrabipour, 2012). It is characterized by simplicity and ability to deal with multiple objectives and solutions. In this method the ideal and non-ideal points represent best and worst solutions, respectively, for each single objective regardless of the other objective's fulfilment, as shown in Figure 6-4.

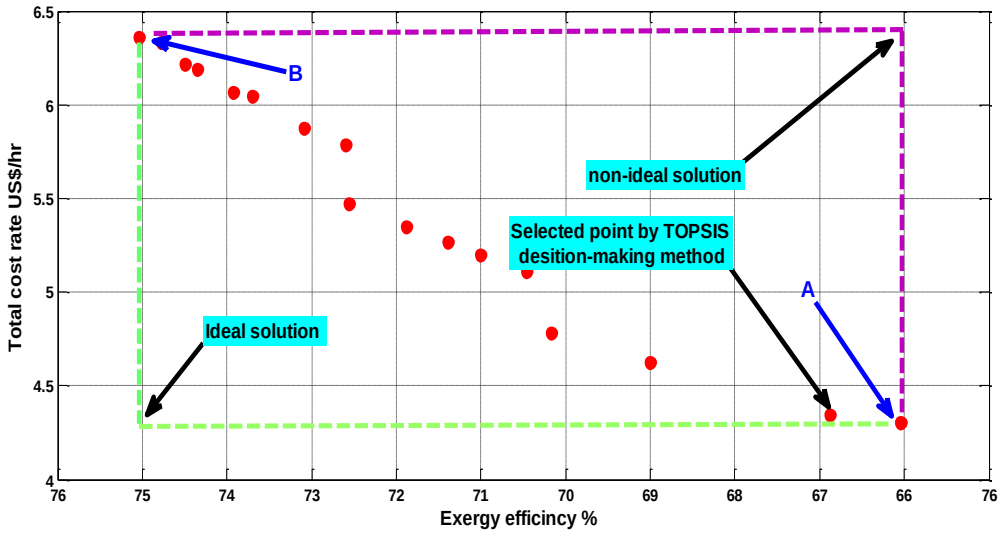

Figure 6-4 The optimum solution obtained from the Pareto frontier using TOPSIS decision making method

The first step in TOPSIS is to obtain the weighted normalized decision matrix of the alternative optimal solutions. The decision matrix values and the weight of each objective (assumed to be 0.5) are shown in Table 6-3. After that, due to the differences in dimensions, all objective functions must be non-dimensionalized, the normalized decision matrix is obtained using Equation 6-1, and the values are shown in Table 6-4.

$$r_{ij} = \frac{x_{ij}}{\sqrt{\sum_i x_{ij}^{\ 2}}} \qquad \text{Equation 6-1}$$

For $i = 1,\ldots\ldots,m$ and $j = 1,\ldots\ldots,n$

Table 6-3 Values of decision matrix

		Exergy efficiency	Cost rate (US$/hr)
Weight		0.5	0.5
Alternative solutions	A1	66.04	4.30
	A2	75.04	6.36
	A3	73.09	5.87
	A4	72.56	5.47
	A5	66.87	4.34
	A6	74.50	6.22
	A7	74.35	6.19
	A8	70.46	5.11
	A9	73.92	6.07
	A10	72.59	5.78
	A11	70.16	4.78
	A12	71.00	5.20
	A13	71.88	5.35
	A14	73.69	6.05
	A15	71.39	5.26
	A16	74.78	6.34
	A17	69.00	4.63

Table 6-4 The normalized (a) and weighted normalized (b) decision matrix.

a

Normalized matrix		
A1	0.222811643	0.188675837
A2	0.253169171	0.278987826
A3	0.24658928	0.257646184
A4	0.244807702	0.239918542
A5	0.225614098	0.190496411
A6	0.251326464	0.272784479
A7	0.250842125	0.27130388
A8	0.23771221	0.224069454
A9	0.249378011	0.266053263
A10	0.244914601	0.25367343
A11	0.236710444	0.20963461
A12	0.239540289	0.227857077
A13	0.242486408	0.23465745
A14	0.248617569	0.265299594
A15	0.240834663	0.230877429
A16	0.252270104	0.277846291
A17	0.232791424	0.202880706

b

Weighted decision matrix.	
0.111405821	0.094337919
0.126584586	0.139493913
0.12329464	0.128823092
0.122403851	0.119959271
0.112807049	0.095248206
0.125663232	0.13639224
0.125421062	0.13565194
0.118856105	0.112034727
0.124689005	0.133026632
0.1224573	0.126836715
0.118355222	0.104817305
0.119770145	0.113928538
0.121243204	0.117328725
0.124308784	0.132649797
0.120417331	0.115438714
0.126135052	0.138923145
0.116395712	0.101440353

Next, the weighted decision matrix is obtained by multiplying each column (objective) with the corresponding weight.

$$v_{ij} = w_i r_{ij}$$ Equation 6-2

The second step is to identify the positive ideal and negative ideal (non-ideal) solutions in the weight normalized matrix. They represent the best (highlighted in green in Table 6-4 b) and the worst values with respect to each objective (highlighted in red).

$$B^{+} = \left(v_1^{+}, \ldots\ldots\ldots v_n^{+}\right)$$ Equation 6-3

$$B^{-} = \left(v_1^{-}, \ldots\ldots\ldots v_n^{-}\right)$$ Equation 6-4

In the third step, the separation of all alternatives from the positive and negative ideal solutions is computed using Equations 6-5 and 6-6, respectively. The results are then listed in Table 6-5and Table 6-6.

$$S_i^+ = \sqrt{\sum_{j=1}^{n} \left(v_{ij} - v_j^+\right)^2} \qquad \text{Equation 6-5}$$

$$S_i^- = \sqrt{\sum_{j=1}^{n} \left(v_{ij} - v_{ij}^-\right)^2} \qquad \text{Equation 6-6}$$

Table 6-5 Separation of each alternative from the positive ideal solution.

Objective1	Objective2	Separation
0.000230395	0	0.015179
0	0.002039064	0.045156
1.08237E-05	0.001189227	0.034642
1.74785E-05	0.000656454	0.02596
0.000189821	8.28623E-07	0.013808
8.48892E-07	0.001768566	0.042064
1.35379E-06	0.001706848	0.04133
5.97294E-05	0.000313177	0.019311
3.59323E-06	0.001496817	0.038735
1.70345E-05	0.001056172	0.03276
6.77224E-05	0.000109818	0.013324
4.64366E-05	0.000383792	0.020742
2.85304E-05	0.000528577	0.023603
5.17927E-06	0.0014678	0.038379
3.8035E-05	0.000445244	0.021984
2.0208E-07	0.001987842	0.044587
0.000103813	5.04446E-05	0.01242

Table 6-6 The separation of each alternative from the negative ideal solution.

Objective1	Objective2	Separation
0	0.002039064	0.045155994
0.000230395	0	0.015178764
0.000141344	0.000113866	0.015975307
0.000120957	0.000381602	0.022417825
1.96344E-06	0.001957683	0.04426789
0.000203274	9.62038E-06	0.014590892
0.000196427	1.47608E-05	0.0145323

5.55067E-05	0.000754007	0.028451953
0.000176443	4.18257E-05	0.01477392
0.000122135	0.000160205	0.016802971
4.82942E-05	0.001202467	0.035366104
6.99619E-05	0.000653588	0.02689889
9.67741E-05	0.000491296	0.024250147
0.000166486	4.68419E-05	0.014605765
8.12073E-05	0.000578653	0.025687738
0.00021695	3.25776E-07	0.014740285
2.4899E-05	0.001448073	0.038379323

The final step is to determine the relative closeness of each alternative to the ideal solution by using Equation 6-7. The value of the relative closeness (TOPSIS scores) is a number between zero and one, and the closer to one, the closer the solution is to the ideal.

$$C_i^+ = \frac{S_i^-}{\left(S_i^- + S_i^+\right)}$$ Equation 6-7

Where:

(S_i^+) is the deviation of the i[th] solution from the positive (ideal) solution.

(S_i^-) is the deviation of the i[th] solution from the negative (non-ideal) solution.

TOPSIS final results are listed in Table 6-7, and the alternative solution A5 has the maximum value of TOPISI scores 0.76247699. Thus this point is selected as the optimum solution. The ideal and non-ideal, alternative solutions and optimal points are all shown in Figure 6-4.

Table 6-7 TOPSIS scores for each alternative.

Alternative	Scores
A1	0.748424215
A2	0.251575785
A3	0.315611125
A4	0.463388551
A5	0.762247699
A6	0.257537971
A7	0.260143157
A8	0.595693498
A9	0.276101364
A10	0.339023867

A11	0.726344811
A12	0.564618152
A13	0.506760478
A14	0.275657567
A15	0.538850805
A16	0.248455038
A17	0.755507761

Table 6-8 shows the values of the design variables and the corresponding values of exergy efficiency, the total cost rate, total cost, coefficient of performance, exergy destruction and solar fraction of the optimum solution.

Table 6-8 Specific characteristics of the optimum solution that have been achieved using the TOPSIS decision making method.

Area (m^2)	Hot tank volume (m^3)	Slope (°)	Cold tank volume (m^3)
50	3.5	30	1.3
Solar fraction for all system		0.4	
Coefficient of performance (COP) of the chiller		0.5	
Exergy destruction (kW)		6.99	
Exergy efficiency (%)		66.84	
Total cost rate (US$/hr)		4.35	
Total cost (US$)		87409.3	

6.8 Analysing the optimum solution

This section will be focused on analysing individual components of the selected optimum solution, in order to identify the parts of the proposed system where high exergy destruction, low exergy efficiency and high total cost rate occur. Figure 6-5 shows the percentage of the exergy destructions for each component, the highest exergy destruction is found to be originated from the solar collector, 41.79%.

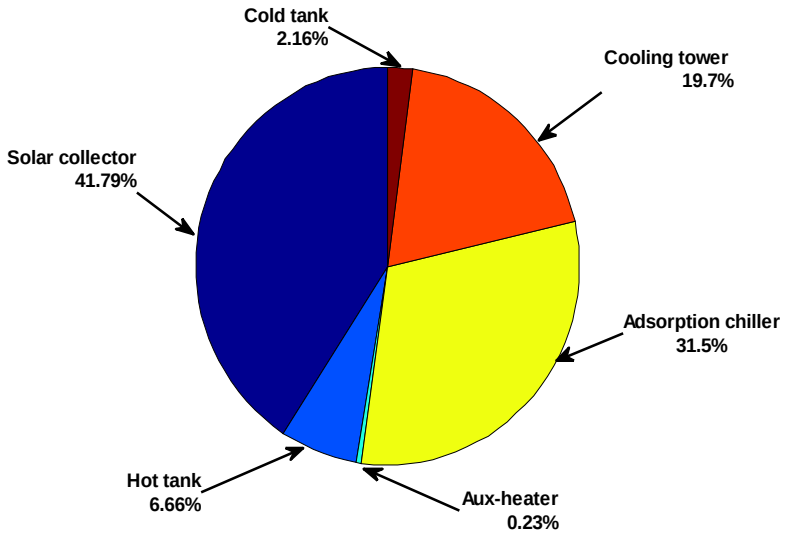

Figure 6-5 Percentage distribution of exergy destructions in the system

As the highest exergy destruction (irreversibility) is located in the solar collector, thus the lowest exergy efficiency should take place in the same component, at 6.41% as shown in Figure 6-6. This means a poor exploitation of a large fraction of the absorbed solar energy in the collector, and similar results have been observed by other researchers (Onan, Ozkan & Erdem, 2010; Zhai *et al.*, 2009).

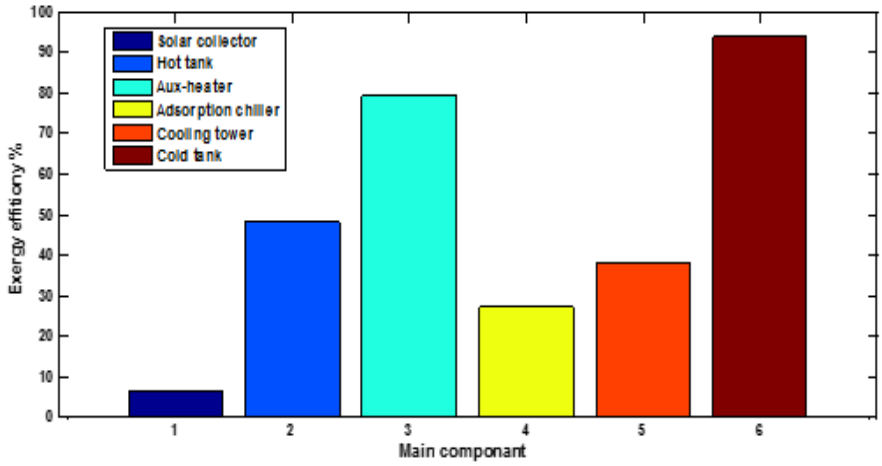

Figure 6-6 Exergy efficiency of each component

The required total cost rates of the system are shown in Figure 6-7. According to the figures, the adsorption chiller was at 49.89% with the highest percentage of cost rates, and the next highest was at the solar collector 32.87%.

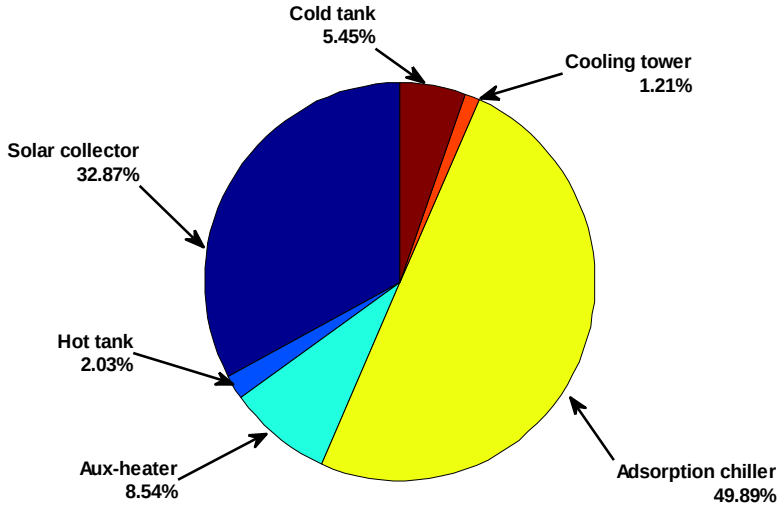

Figure 6-7 percentage distribution of the total cost rate (US$/hr) for the main components in the system

All values in Figures 6-5, 6-6 and 6-7 are presented in Table 6-9. The highest exergy destruction and exergy efficiency was found in solar collector (2.922kW) and cold storage tank (93.77%), respectively. Whereas the highest total cost rate (operation cost rate plus investment cost rate) was at the adsorption chiller (2.140US$/hr), and the next highest was at the solar collector (1.411US$/hr).

Table 6-9 Specific characteristics of the optimum solution that have been achieved using the TOPSIS decision making method.

Component	Exergy destruction (kW)	Exergy efficiency (%)	Total Cost rate (US$/hr)
Solar collector	2.922	6.41	1.411
Hot storage tank	0.465	57.99	0.087
Auxiliary heater	0.016	87.57	0.367
Adsorption chiller	2.205	27.12	2.140
Cooling tower	1.381	38.15	0.052
Cold tank	0.015	93.77	0.233

6.9 Comparison with original system

After obtaining the optimal design parameter values and analysing each component of the optimum system, a comparison has been made with the original system that was installed for the Solar House in Baghdad (A. Al-Karaghouli, 1989; Joudi & Abdul-Ghafour, 2003). Table 6-10 shows the proposed system specifications and that of the original system. The capacity of the chiller, the area of the solar collector and the volume of the hot water storage tank are all reduced substantially for the same building. This in turn can be interpreted as a reduction in investment and operation costs, which was one of the main objectives of this study.

Table 6-10 A comparison between the proposed system and the original system.

Comparison of the proposed system with original system			
Main component		Original system	Proposed(obtained from GA)
Chiller type and size		Absorption chiller 10 TR (35kW)	Adsorption chiller 5TR (18kW)
Collector	Type	Flat plate	Evacuated tube
	Area	243m²	50m³
	Orientation	South east 22.5^0	South
	Slope	15.6^0	30^0
Hot tank volume		20m³	3.5m³
Cold tank volume		-	1.3m³
Solar fraction		0.51	0.4
Investment cost		-	87409.3US$
Coefficient of performance		0.443	0.5

The original system which was installed for the Solar House building in Baghdad has used a 10TR absorption chiller driven by $243m^2$ flat plate collector and $20m^3$ volume of hot storage tank. While in present study, a solar adsorption cooling system for the same building has been used. The results showed that the solar adsorption system driven by evacuated tube solar collector and integrated with the hot and cold storage tank gives a smaller size than the original system, which in turn can be interpreted as a reduction in the investment and the operation cost of the system. The solar fraction for original system was 0.51 while for proposed system was 0.4 and the confection of performance of the original system and the proposed system was o.443 and 0.5, respectively.

6.10 The payback period

In order to compare solar adsorption system with other alternatives, the payback period was calculated. Payback period estimates the time needed to cumulative fuel savings to the total initial investment costs. In other words, it represents how long it will take to get the initial investment costs back by savings in fuel (Duffie & Beckman, 1980).

The payback period can be estimated using Equation 6-8 (Al-Alili et al., 2012):-

$$N_p = \frac{\ln\left(\frac{C_{\text{int}} * if}{Q_{usful} * C_{elec}}\right)}{\ln(1+if)} \qquad \text{Equation 6-8}$$

Where:-

(C_{int}) is the initial investment cost (US$).

(if) is the inflation rate (10% (Al-Alili *et al.*, 2012)).

$(Q_{usful})$is the useful energy of the solar collector (kW.hr).

(C_{elec}) is the electricity price (0.02 US$/kW.hr in Iraq 2014).

The resulting financial payback period was a long time (31 years), is because of the high initial cost of the solar adsorption cooling system. However, by reducing the cost of the system and government incentives could be made more economic in the future. A similar result (long payback period) was found in previous studies (Cheng Hin & Zmeureanu, 2014; Leckner & Zmeureanu, 2011).

6.11 Summary

In this chapter, a multi-objective optimization approach is presented and illustrated by applying it to the design of a solar adsorption system in Baghdad. The approach, coupling genetic algorithm in MATAB with TRNSYS, aims to maximize the exergy efficiency and minimize the total cost rate of the system in order to find the optimum configuration of the system. A set of optimal solutions are found through the final achieved Pareto front. Technique for Order Performance by Similarity to Ideal Solution (TOPSIS) method is used to find the final optimal solution. The characteristics of the optimum solution are then presented with analysis on individual components of the proposed system. Areas where high exergy

destruction, low exergy efficiency and high total cost rate occur have been identified. Finally, the payback period of the system has been estimated.

Chapter Seven

Conclusions and future work

7.1 Conclusions

In the present study, an environmentally friendly solar adsorption cooling system was modelled and simulated in TRNSYS software. The simulation was carried out using the Typical Meteorological Year (TMY2) data for Baghdad, Iraq. The proposed system was analysed and assessed to find the solar fraction, exergy destruction and exergy efficiency of the system, and the operation and investment cost rates for the system were also techno-economically evaluated.

A parametric study has been done on the system by changing several key parameters (collector area, hot storage tank volume, collector slope and cold storage tank volume). The effects of changing these parameters on the performance of the system (solar fraction, investment cost rate, operation cost rate, exergy destruction and exergy efficiency) were investigated and can be summed up as follows: -

- Solar fraction increases with an increase in collector area, while it generally decreases with an increase in hot storage tank volume for each given area.

- The operation cost rate is more sensitive than the investment cost rate when changing the volume of hot storage tank.

- Small collector areas should be recommended if low exergy destruction was to be desired.

- For large area collectors, increasing the storage volume can be a more effective improvement on system exergy efficiency.

- Solar fraction is more sensitive to hot storage tank volume than cold storage tank volume; there is no advantage of cold storage greater than $1m^3$.

- The optimal inclination angle of solar collectors is directly related to the collector area, which is essential to decrease the operation cost rate.

-There is no advantage of inclination angle greater than 30^{o} on investment cost rate, exergy destruction and exergy efficiency.

Furthermore, the system was optimized by employing multi-objective Genetic Algorithm optimization. The Pareto front optimal set solutions were achieved from multi-objective optimization of the system, integrating with the two objective functions, namely exergy efficiency and total cost rate. As all achieved points from the Pareto front can be chosen as the optimal design point, a process of decision-making is important in order to find the final solution of the system. Technique for Order Performance by Similarity to Ideal Solution (TOPSIS) decision making method was applied to obtain the final optimum design. The chosen optimum design has a maximum value of TOPSIS score 0.76247699, while the exergy efficiency and the cost rate were 4.34 US$/hr and 66.87%, respectively. The coefficient of the performance of the proposed system was 0.5.

The optimum solution was then analysed in order to identify the parts of the proposed system which have high exergy destruction, low exergy efficiency and high total cost rate. The results demonstrated that the highest exergy destruction (irreversibility) and lowest exergy efficiency is located in the solar collector (41.79% and 6.4%, respectively), while the highest percentage of the cost rate was for the adsorption chiller (49.89%). In addition, a comparison has been made with the original system which was installed for the Solar House building in Baghdad. The results showed that the solar adsorption system driven by evacuated tube collector and integrated with the hot and cold storage tank gives a smaller size than the original system, which in turn can be interpreted as a reduction in the investment and the operation cost of the system.

To complete the investigation, the financial payback period has been estimated, and it is too long, (31year financial payback period) to be economically feasible. The reasons for such a long payback period were identified as the high cost of solar adsorption cooling systems and the low price of electricity in Iraq. By reducing the cost of the system, government incentives, and most importantly introducing the GHG emission tax rate, the system could become more environmentally and economically attractive; and this technology may even beat traditional cooling systems economically, as was found in Gebreslassie (2010).

7.2 Future work

The solar adsorption cooling system needs more development, especially in terms of costs, to make the system more attractive to the consumer. In the future, this study can be extended to include the cost of exergy rate and the environmental analysis in order to drive down the costs further. In addition, control strategies for the system can be developed in order to achieve a more efficient system. Furthermore, the proposed system can be assessed for different building types such as office buildings, as well as in different cities in Iraq. Further recommendations include a comparison with the conventional air conditioning system to show how the proposed model consumes less electricity and is more environmentally friendly.

References

A. Al-Karaghouli, N. A.-H., W. Al-Sinan (1989) 'Iraqi solar house cooling season performance evaluation'. *Solar & Wind Technology*, 6 (1). pp 29-40.

Abbaspour, M. & Saraei, A. (2015) 'Thermoeconomic Analysis and Multi-Objective Optimization of a LiBr-Water Absorption Refrigeration System'. *Int. J. Environ. Res*, 9 (1). pp 61-68.

Abdulsada, G. K. & Salih, T. W. M. (2015) 'Experimental Study to Evaluate the Performance of Iraqi Passive House in Summer Season'. *Journal of Energy and Power Engineering*, pp 386-392.

Abu Hamdeh, N. H. & Al-Muhtaseb, M. t. A. (2010) 'Optimization of solar adsorption refrigeration system using experimental and statistical techniques'. *Energy Conversion and Management*, 51 (8). pp 1610-1615.

Ahmadi, M. H., Sayyaadi, H., Mohammadi, A. H. & Barranco-Jimenez, M. A. (2013) 'Thermo-economic multi-objective optimization of solar dish-Stirling engine by implementing evolutionary algorithm'. *Energy Conversion and Management*, 73 pp 370-380.

Al-Alili, A., Hwang, Y., Radermacher, R. & Kubo, I. (2010) 'Optimization of a solar powered absorption cycle under Abu Dhabi's weather conditions'. *Solar Energy*, 84 (12). pp 2034-2040.

Al-Alili, A., Islam, M. D., Kubo, I., Hwang, Y. & Radermacher, R. (2012) 'Modeling of a solar powered absorption cycle for Abu Dhabi'. *Applied Energy*, 93 pp 160-167.

Al-Helal, A. (2015) 'Solar Energy as an Alternative Energy than the Conventional Means of Electricity Generation in Iraq'. *International Journal of Inventive Engineering and Sciences*, 3 (2).

Al-Salihi, A. M., M.M. Kadum and A.J. Mohammed (2010) 'Estimation of Global Solar Radiation on Horizontal Surface Using Routine Meteorological Measurements for Different Cities in Iraq'. *Asian J. Sci. Res.*, 3 (4). pp 240-248.

Alam, K. C. A., Saha, B. B. & Akisawa, A. (2013) 'Adsorption cooling driven by solar collector: A case study for Tokyo solar data'. *Applied Thermal Engineering*, 50 (2). pp 1603-1609.

Alam, K. C. A., Saha, B. B., Kang, Y. T., Akisawa, A. & Kashiwagi, T. (2000) 'Heat exchanger design effect on the system performance of silica gel adsorption refrigeration systems'. *International Journal of Heat and Mass Transfer*, 43 (24). pp 4419-4431.

Alasady, A. M. A. (2011) 'Solar energy the suitable energy alternative for Iraq beyond oil'. *International Conference on Petroleum and Sustainable Development26*. Singapore: IACSIT Press.

Aman, J., Ting, D. S. K. & Henshaw, P. (2014) 'Residential solar air conditioning: Energy and exergy analyses of an ammonia–water absorption cooling system'. *Applied Thermal Engineering*, 62 (2). pp 424-432.

Aminyavari, M., Najafi, B., Shirazi, A. & Rinaldi, F. (2014) 'Exergetic, economic and environmental (3E) analyses, and multi-objective optimization of a CO2/NH3 cascade refrigeration system'. *Applied Thermal Engineering*, 65 (1–2). pp 42-50.

Anyanwu, E. E. & Ogueke, N. V. (2005) 'Thermodynamic design procedure for solid adsorption solar refrigerator'. *Renewable Energy*, 30 (1). pp 81-96.

Baghernejad, A. & Yaghoubi, M. (2012) *Exergoeconomic Analysis and Optimization of Solar Thermal Power Plants.* INTECH Open Access Publisher.

Baiju, V. & Muraleedharan, C. (2012) 'Exergy Assessment of Single Stage Solar Adsorption Refrigeration System Using ANN'. *ISRN Mechanical Engineering*, 2012 pp 10.

Baiju, V. & Muraleedharan, C. (2013) 'Energy and exergy analysis of solar hybrid adsorption refrigeration system'. *International Journal of Sustainable Engineering*, 6 (4). pp 289-300.

Baniyounes, A. M., Liu, G., Rasul, M. G. & Khan, M. M. K. (2013) 'Comparison study of solar cooling technologies for an institutional building in subtropical Queensland, Australia'. *Renewable and Sustainable Energy Reviews*, 23 pp 421-430.

Behbahani-nia, A. & Sayfikar, M. (2013) 'Study of the performance of a solar adsorption cooling system'. *Energy Equipment and Systems*, 1 (1). pp 75-90.

Bejan, A. (2006) *Advanced Engineering Thermodynamics.* Wiley.

Caliskan, H., Dincer, I. & Hepbasli, A. (2012) 'Thermodynamic analyses and assessments of various thermal energy storage systems for buildings'. *Energy Conversion and Management*, 62 (0). pp 109-122.

Caliskan, H., Dincer, I. & Hepbasli, A. (2013) 'Thermoeconomic analysis of a building energy system integrated with energy storage options'. *Energy Conversion and Management*, 76 pp 274-281.

Cheng Hin, J. N. & Zmeureanu, R. (2014) 'Optimization of a residential solar combisystem for minimum life cycle cost, energy use and exergy destroyed'. *Solar Energy*, 100 pp 102-113.

Clausse, M., Alam, K. C. A. & Meunier, F. (2008) 'Residential air conditioning and heating by means of enhanced solar collectors coupled to an adsorption system'. *Solar Energy*, 82 (10). pp 885-892.

Davis, L. W. & Gertler, P. J. (2015) 'Contribution of air conditioning adoption to future energy use under global warming'. *Proceedings of the National Academy of Sciences*, 112 (19). pp 5962-5967.

Davis, P. (2014) *SolarKeymark Certificate.* Fakhraldin, S.

Desideri, U., Proietti, S. & Sdringola, P. (2009) 'Solar-powered cooling systems: Technical and economic analysis on industrial refrigeration and air-conditioning applications'. *Applied Energy*, 86 (9). pp 1376-1386.

Dincer, I. & Kanoglu, M. (2010) *Refrigeration Systems and Applications.* Wiley.

Dincer, I. & Rosen, M. A. (2001) 'Energetic, environmental and economic aspects of thermal energy storage systems for cooling capacity'. *Applied Thermal Engineering*, 21 (11). pp 1105-1117.

Dincer, I. & Rosen, M. A. (2011) *Thermal Energy Storage: Systems and Applications.* Wiley.

Duffie, J. A. & Beckman, W. A. (1980) *Solar engineering of thermal processes.* vol. 3. Wiley New York etc.

Eicker, U. & Pietruschka, D. (2009) 'Design and performance of solar powered absorption cooling systems in office buildings'. *Energy and Buildings*, 41 (1). pp 81-91.

El-Sharkawy, I. I., AbdelMeguid, H. & Saha, B. B. (2013) 'Towards an optimal performance of adsorption chillers: Reallocation of adsorption/desorption cycle times'. *International Journal of Heat and Mass Transfer*, 63 (0). pp 171-182.

Fernandes, M., Brites, G., Costa, J., Gaspar, A. & Costa, V. (2014) 'Review and future trends of solar adsorption refrigeration systems'. *Renewable and Sustainable Energy Reviews*, 39 pp 102-123.

Fisenko, S. P., Brin, A. A. & Petruchik, A. I. (2004) 'Evaporative cooling of water in a mechanical draft cooling tower'. *International Journal of Heat and Mass Transfer*, 47 (1). pp 165-177.

Fong, K. F., Chow, T. T., Lee, C. K., Lin, Z. & Chan, L. S. (2010) 'Comparative study of different solar cooling systems for buildings in subtropical city'. *Solar Energy*, 84 (2). pp 227-244.

Gebreslassie, B. H. (2010) *Optimization of Environmentilly Friendly Solar Assisted Absorption Cooling Systems*. Universitat Rovira I Virgili.

Gebreslassie, B. H., Guillén-Gosálbez, G., Jiménez, L. & Boer, D. (2009) 'Design of environmentally conscious absorption cooling systems via multi-objective optimization and life cycle assessment'. *Applied Energy*, 86 (9). pp 1712-1722.

Gebreslassie, B. H., Medrano, M. & Boer, D. (2010) 'Exergy analysis of multi-effect water–LiBr absorption systems: From half to triple effect'. *Renewable Energy*, 35 (8). pp 1773-1782.

Gerstler, W. & Tang, C.-J. (2011) 'A Lithium Bromide Absorption Chiller with Cold Storage', *11th International Sorption Heat Pump Conference (ISHPC11)*. Padua, Italy DTIC Document.

'GoModel Solar'. [Online]. Available at: http://solargis.info/doc/free-solar-radiation-maps-GHI (Accessed: 28th Sept 2015).

Hang, Y., Du, L., Qu, M. & Peeta, S. (2013) 'Multi-objective optimization of integrated solar absorption cooling and heating systems for medium-sized office buildings'. *Renewable Energy*, 52 pp 67-78.

Hang, Y., Qu, M. & Zhao, F. (2011) 'Economical and environmental assessment of an optimized solar cooling system for a medium-sized benchmark office building in Los Angeles, California'. *Renewable Energy*, 36 (2). pp 648-658.

Hang, Y. a. Q., Ming (2010) 'The impact of hot and cold storages on a solar absorption cooling system for an office building'. *International High Performance Buildings*. School of Mechanical Engineering, pp 48.

Hassan, H. Z. & Mohamad, A. A. (2012) 'A review on solar-powered closed physisorption cooling systems'. *Renewable and Sustainable Energy Reviews*, 16 (5). pp 2516-2538.

Hassan, H. Z., Mohamad, A. A. & Bennacer, R. (2011) 'Simulation of an adsorption solar cooling system'. *Energy*, 36 (1). pp 530-537.

Hepbasli, A. (2007) 'Exergetic modeling and assessment of solar assisted domestic hot water tank integrated ground-source heat pump systems for residences'. *Energy and Buildings*, 39 (12). pp 1211-1217.

Hepbasli, A. (2008) 'A key review on exergetic analysis and assessment of renewable energy resources for a sustainable future'. *Renewable and Sustainable Energy Reviews*, 12 (3). pp 593-661.

Hepbasli, A. (2010) 'A review on energetic, exergetic and exergoeconomic aspects of geothermal district heating systems (GDHSs)'. *Energy Conversion and Management*, 51 (10). pp 2041-2061.

InvenSor (2013) 'Adorption Chiller: INVENSOR HTC 18 Plus Data Sheet'.[in. Available at: http://www.invensor.com/en/pdf/InvenSor_Datasheet_HTC18_EN_Web.pdf (Accessed:InvenSor 16th Jan 2015).

Istepanian, H. H. (2014) 'Iraq's Electricity Crisis'. *The Electricity Journal*, 27 (4). pp 51-69.

Jakobe, P. K. U. (2014) *Solar Cooling.* ed. jackson, F., Earthscan expert. Routledge:

Januševičius, K., Streckienė, G. & Misevičiūtė, V. (2015) 'Simulation and Analysis of Small-Scale Solar Adsorption Cooling System for Cold Climate'.

Joudi, K. A. & Abdul-Ghafour, Q. J. (2003) 'Development of design charts for solar cooling systems. Part I: computer simulation for a solar cooling system and development of solar cooling design charts'. *Energy Conversion and Management*, 44 (2). pp 313-339.

Kalogirou, S. A. (2004) 'Solar thermal collectors and applications'. *Progress in Energy and Combustion Science*, 30 (3). pp 231-295.

Klein, S. A., Beckman, W. A. & Mitchell, J. W. (2014a) *TRNSYS 17 Mathematical Reference*.

Klein, S. A., Beckman, W. A. & Mitchell, J. W. (2014b) *TRNSYS17-Main Menu.*

Kwak, H.-Y., Kim, D.-J. & Jeon, J.-S. (2003) 'Exergetic and thermoeconomic analyses of power plants'. *Energy*, 28 (4). pp 343-360.

Leckner, M. & Zmeureanu, R. (2011) 'Life cycle cost and energy analysis of a Net Zero Energy House with solar combisystem'. *Applied Energy*, 88 (1). pp 232-241.

Li, Z. F. & Sumathy, K. (2001) 'Experimental studies on a solar powered air conditioning system with partitioned hot water storage tank'. *Solar Energy*, 71 (5). pp 285-297.

Martínez, P. J., Martínez, J. C. & Lucas, M. (2012) 'Design and test results of a low-capacity solar cooling system in Alicante (Spain)'. *Solar Energy*, 86 (10). pp 2950-2960.

Mateus, T. & Oliveira, A. C. (2009) 'Energy and economic analysis of an integrated solar absorption cooling and heating system in different building types and climates'. *Applied Energy*, 86 (6). pp 949-957.

Milani, D. & Abbas, A. (2016) 'Multiscale modeling and performance analysis of evacuated tube collectors for solar water heaters using diffuse flat reflector'. *Renewable Energy*, 86 pp 360-374.

'Ministry of Electricity of Iraq'. [Online]. Available at: http://www.moelc.gov.iq/ (Accessed: 1st Sept 2014).

Morrison, G., Budihardjo, I. & Behnia, M. (2004) 'Water-in-glass evacuated tube solar water heaters'. *Solar Energy*, 76 (1). pp 135-140.

Navidbakhsh, M., Shirazi, A. & Sanaye, S. (2013) 'Four E analysis and multi-objective optimization of an ice storage system incorporating PCM as the partial cold storage for air-conditioning applications'. *Applied Thermal Engineering*, 58 (1–2). pp 30-41.

Onan, C., Ozkan, D. B. & Erdem, S. (2010) 'Exergy analysis of a solar assisted absorption cooling system on an hourly basis in villa applications'. *Energy*, 35 (12). pp 5277-5285.

Ozgen, C. (2008) *Thermodynamics and Economic Analysis of a Solar Thermal Powerd Adsorption Cooling System*. MSc thesis. Middle East Technical University.

Petela, R. (2003) 'Exergy of undiluted thermal radiation'. *Solar Energy*, 74 (6). pp 469-488.

Rafique, M. M., Gandhidasan, P., Al-Hadhrami, L. M. & Rehman, S. (2016) 'Energy, Exergy and Anergy Analysis of a Solar Desiccant Cooling System'. *Journal of Clean Energy Technologies*, 4 (1). pp 78-83.

Sadeghlu, A., Yari, M., Mahmoudi, S. M. S. & Dizaji, H. B. (2014) 'Performance evaluation of Zeolite 13X/CaCl2 two-bed adsorption refrigeration system'. *International Journal of Thermal Sciences*, 80 (0). pp 76-82.

Saha, B. B., El-Sharkawy, I. I., Chakraborty, A. & Koyama, S. (2007) 'Study on an activated carbon fiber–ethanol adsorption chiller: Part I – system description and modelling'. *International Journal of Refrigeration*, 30 (1). pp 86-95.

Sanaye, S. & Shirazi, A. (2013) 'Thermo-economic optimization of an ice thermal energy storage system for air-conditioning applications'. *Energy and Buildings*, 60 pp 100-109.

Şasmaz, T. (2011) *Thermodynamic Analysis of a Solar Assisted Adsorption System*. MSc thesis. Near East University

Sayyaadi, H. & Mehrabipour, R. (2012) 'Efficiency enhancement of a gas turbine cycle using an optimized tubular recuperative heat exchanger'. *Energy*, 38 (1). pp 362-375.

Shirazi, A., Aminyavari, M., Najafi, B., Rinaldi, F. & Razaghi, M. (2012) 'Thermal–economic–environmental analysis and multi-objective optimization of an internal-reforming solid oxide fuel cell–gas turbine hybrid system'. *International Journal of Hydrogen Energy*, 37 (24). pp 19111-19124.

Shirazi, A., Najafi, B., Aminyavari, M., Rinaldi, F. & Taylor, R. A. (2014) 'Thermal–economic–environmental analysis and multi-objective optimization of an ice thermal energy storage system for gas turbine cycle inlet air cooling'. *Energy*, 69 (0). pp 212-226.

Thornton, J. W., Bradley, D. E. & McDowell, T. P. (2014) *TESSLibs 17 HVAC Library Mathematical Reference.* Available.

'Trading Economics'. [Online]. Available at: http://www.tradingeconomics.com/iraq/interest-rate (Accessed: 1st Sept 2015).

'TRNSYS'. [Online]. Available at: http://www.trnsys.com/ (Accessed: 25th Sept 2015).

Tsatsaronis, G. (1993) 'Thermoeconomic analysis and optimization of energy systems'. *Progress in Energy and Combustion Science*, 19 (3). pp 227-257.

Tsoutsos, T., Aloumpi, E., Gkouskos, Z. & Karagiorgas, M. (2010) 'Design of a solar absorption cooling system in a Greek hospital'. *Energy and Buildings*, 42 (2). pp 265-272.

Tyagi, V. V., Rahim, N. A. A., Rahim, N. A. & Selvaraj, J. A. L. (2013) 'Progress in solar PV technology: Research and achievement'. *Renewable and Sustainable Energy Reviews*, 20 pp 443-461.

Wang, L. W., Wang, R. Z. & Oliveira, R. G. (2009) 'A review on adsorption working pairs for refrigeration'. *Renewable and Sustainable Energy Reviews*, 13 (3). pp 518-534.

Wang, R., Wang, L. & Wu, J. (2014) *Adsorption refrigeration technology: theory and application.* John Wiley & Sons.

Wang, R. Z., Ge, T. S., Chen, C. J., Ma, Q. & Xiong, Z. Q. (2009) 'Solar sorption cooling systems for residential applications: Options and guidelines'. *International Journal of Refrigeration*, 32 (4). pp 638-660.

White, J. (2013) *CFD simulation of silica gel and water adsorbent beds used in adsorption cooling system*. phD thesis. University of Birmingham.

Yong, L. & Sumathy, K. (2004) 'Modeling and simulation of a solar powered two bed adsorption air conditioning system'. *Energy Conversion and Management*, 45 (17). pp 2761-2775.

Zhai, H., Dai, Y. J., Wu, J. Y. & Wang, R. Z. (2009) 'Energy and exergy analyses on a novel hybrid solar heating, cooling and power generation system for remote areas'. *Applied Energy*, 86 (9). pp 1395-1404.

Zhai, X. Q. & Wang, R. Z. (2009) 'A review for absorbtion and adsorbtion solar cooling systems in China'. *Renewable and Sustainable Energy Reviews*, 13 (6–7). pp 1523-1531.